Fourier Transform Spectroscopy of the O_2 Herzberg Bands

II. Band Oscillator Strengths and Transition Moments

M.-F. Mérienne,* A. Jenouvrier,* B. Coquart,* M. Carleer,† S. Fally,† R. Colin,†
A. C. Vandaele,‡ and C. Hermans‡

*Groupe de Spectrométrie Moléculaire et Atmosphérique, UPRESA 6089, UFR Sciences, Moulin de la Housse, B. P. 1039, 51687 Reims Cedex 2, France;
†Service de Chimie Physique Moléculaire, Université Libre de Bruxelles, CP 160/09, Av. F. D. Roosevelt 50, B-1050 Brussels, Belgium; and
‡Institut d'Aéronomie Spatiale de Belgique, 3, Av. Circulaire, B-1180 Brussels, Belgium

From absorption spectra obtained at high resolution by coupling a Fourier transform spectrometer to a long-path multiple reflection cell [A. Jenouvrier, M.-F. Mérienne, B. Coquart, M. Carleer, S. Fally, A. C. Vandaele, C. Hermans, and R. Colin, *J. Mol. Spectrosc.* **198,** 136–162 (1999)] the intensities of the O_2 Herzberg bands ($A^3\Sigma_u^+ - X^3\Sigma_g^-$, $c^1\Sigma_u^- - X^3\Sigma_g^-$, $A'^3\Delta_u - X^3\Sigma_g^-$) have been studied at ambient temperature. The integrated cross section values are given for the lines of the ($v'-0$) bands in the $A^3\Sigma_u^+ - X^3\Sigma_g^-$, $c^1\Sigma_u^- - X^3\Sigma_g^-$, and $A'^3\Delta_u - X^3\Sigma_g^-$ transitions with $v' = 0-11$, $v' = 2-19$, and $v' = 2-12$, respectively. The band oscillator strengths have been deduced and transition moments have been calculated. The total absorption values in the region of the Herzberg bands together with the photoabsorption values determined previously above the dissociation limit can be modeled by a single curve, in agreement with the continuity relationship of the cross sections through the dissociation limit. © 2000 Academic Press

INTRODUCTION

Absorption of solar radiation below $\lambda < 242$ nm by molecular O_2 leads to its dissociation into $O(^3P)$ atoms which in turn can combine with O_2 to give ozone molecules. The limit of dissociation at 242 nm corresponds to the convergence of the three electronic transitions $A^3\Sigma_u^+ - X^3\Sigma_g^-$, $c^1\Sigma_u^- - X^3\Sigma_g^-$, and $A'^3\Delta_u - X^3\Sigma_g^-$, known as the Herzberg band systems I, II, and III, respectively (*1, 2*). To quantify correctly the absorption into the continuum (*3*), it is necessary to know accurate parameters for the states involved and the related transition moments. For this reason, numerous studies have been devoted to these transitions (*4–10*). Recently, a renewed interest in the study of these transitions was generated by the extensive use of optical techniques such as DOAS (differential optical absorption spectroscopy) to detect and measure the concentration of ozone and other species in the atmosphere. In the UV region, the O_2 contribution results from the discrete Herzberg bands due to molecular oxygen and from diffuse bands (the Wulf bands) due to collisional processes (*11*). In contrast to the Herzberg bands, the Wulf bands have a cross section that depends on the total pressure (*12*). For atmospheric measurements it is therefore necessary to know accurate values of the cross sections in the Herzberg bands. As these are electric-dipole forbidden, their intensities are weak and long absorption paths are required for their observation in close-to-atmospheric conditions.

Previous, high-resolution recordings by photographic

(*4–6*) and photoelectric (*7–10*) techniques have allowed the extension of the vibrational and rotational assignments given by Herzberg (*1, 2*) in the three transitions and the improvement of the molecular parameters of the upper states. We have reported in a recent paper (*13*), hereafter referred to as Paper I, the observation and the assignments of new lines, particularly in the $A'-X$ transition and given new information on the $c-A$ interactions. The existence of a weakly bound $^3\Pi_u$ state perturbing the $A^3\Sigma_u^+$ state in the $v = 11$ level close to the dissociation threshold was also confirmed.

Intensity measurements were performed for these systems; the earlier ones were obtained from photographic measurements (*14, 15*) for a few bands of the most intense $A-X$ transitions. Later, modern techniques such as cavity ring-down spectroscopy (CRDS) and Fourier transform spectroscopy (FTS) allowed the reinvestigation of the intensities in the $A-X$ bands (*7, 8, 10, 16–20*). Four (*7, 18, 21, 22*) and three (*7, 18, 23*) studies also report on the intensities of the $c-X$ and $A'-X$ transitions, respectively; two of them (*18, 23*) are theoretical papers.

In the present paper, based on the same FTS spectra reported in Paper I, we present measurements of the intensities of the lines for the three Herzberg band systems from which oscillator strengths and transition moments are calculated. The corresponding total cross section below the dissociation limit is determined and is in agreement with the photodissociation cross section currently accepted (*24*).

TABLE 1a
Integrated Cross Sections of Lines in the $A–X$ $(v'–0)$ Bands of O_2

0-0 Band

N	$^QQ_{11}$	$^QR_{12}$	$^QR_{23}$	$^OP_{21}$	$^OP_{32}$
1	0.2*		0.1*		
3	0.2	0.1	0.1	0.1	0.1
5	0.2	0.2	0.2*	0.1*	0.2
7	0.3	0.2	0.3*	0.2*	0.3
9	0.2*	0.4	0.2*	0.2*	0.2*
11	0.3	0.2	0.2	0.2	0.2
13	0.2	0.2	0.2	0.2	0.2
15	0.2	0.2*		0.2*	0.2
17	0.1			0.2*	
				0.1	

$^QQ_{11}(1)$, $^QR_{23}(1)$ $^QR_{23}(7)$, $^OP_{21}(7)$
$^QQ_{11}(9)$, $^OP_{32}(9)$ $^QR_{23}(9)$, $^OP_{21}(9)$
$^QR_{12}(15)$, $^PP(1)$ c3 $^OP_{21}(15)$, $^RQ(5)$ c3
$^QR_{23}(5)$, $^QP_{21}(5)$

1-0 Band

N	$^QQ_{11}$	$^QQ_{22}$	$^QQ_{33}$	$^QR_{12}$	$^QR_{23}$	$^OP_{21}$	$^OP_{32}$	$^OP_{12}$	$^OP_{23}$	$^SR_{21}$
1	1.1*	0.6		0.6	0.1*	0.4				
3	1.3	0.2		1.1	1.2	1.1	0.7*	0.3*	0.1*	
5	1.9	0.3	0.3	1.6	1.6*	1.5*	1.1	0.4	0.2	
7	2.2	0.4	0.5	2.0	1.9*	1.8*	1.4	0.3	0.2	0.2*
9	2.2*		0.4	1.9	1.9*	1.8*	1.4*	0.3		0.3
11	2.1	0.4	0.4	1.6	1.5	1.7	1.4	0.3		0.2
13	1.8	0.3	0.2	1.4	1.3	1.4	1.2	0.2		
15	1.5	0.2		1.2	0.9	1.0	1.0	0.2		
17	1.1			0.8	0.6	0.8	0.7			
19	0.8			0.6	0.5	0.4	0.6			
21	0.5			0.2	0.3	0.3*	0.2			
23	0.3			0.2*	0.1	0.2				

$^QQ_{11}(1)$, $^QR_{23}(1)$ $^QR_{23}(5)$, $^OP_{21}(5)$ $^OP_{21}(21)$, $^RR(9)$ c4
$^QQ_{11}(9)$, $^OP_{32}(9)$ $^QR_{23}(7)$, $^OP_{21}(7)$ $^OP_{32}(3)$, $^SR_{21}(7)$
$^QR_{12}(23)$, $^RQ(13)$ c4 $^QR_{23}(9)$, $^OP_{21}(9)$ $^OP_{12}(3)$, $^OP_{23}(3)$

2-0 Band

N	$^QQ_{11}$	$^QQ_{22}$	$^QQ_{33}$	$^QR_{12}$	$^QR_{23}$	$^OP_{21}$	$^OP_{32}$	$^OP_{12}$	$^OP_{23}$	$^SR_{21}$
1	3.0*	2.1		2.5	2.0*	2.3*	0.8			
3	5.3	1.2	1.0	5.6*	6.2*	4.5*	3.2	2.1*	0.4*	
5	8.6	1.0	1.6	7.3*	7.2*	6.7*	5.5*	2.2*	0.5	2.0
7	9.5*	1.1	1.8	9.0	8.0*	8.0*	6.7	1.6	0.5	0.5
9	10.3*	1.0*	1.5	8.3	9.5*	9.1*	6.8*	1.4	0.5	0.4
11	9.4	1.0*	1.2	7.8	7.1	6.9*	6.0	1.0	0.5	0.4*
13	8.5	0.9	1.0	6.5	5.9	6.1	5.8	0.8	0.4	0.4*
15	7.1	0.9	0.6	4.5	4.4	4.2	4.2	0.5	0.3	0.5*
17	5.4	0.9	0.3	3.2	3.4	3.1	3.0	0.3*	0.3	0.2
19	3.2*	0.6		2.0	1.8	2.2	2.0	0.2		
21	2.1	0.5		1.3	1.3	1.2	1.0			
23	1.5	0.4		0.8*	0.6	0.7	0.8			
25	0.9			0.3	0.5	0.5	0.4			
27	0.3			0.2			0.3			
29	0.3									

$^QQ_{11}(1)$, $^QR_{23}(1)$ $^QR_{12}(23)$, $^RQ(3)$ c5 $^OP_{32}(5)$, $^RQ_{21}(17)$ A'3
$^QQ_{11}(9)$, $^OP_{32}(9)$ $^QR_{23}(3)$, $^OP_{21}(3)$, $^QQ_{22}(15)$ A'3 $^OP_{12}(5)$, $^SR_{21}(11)$
$^QQ_{11}(19)$, $^RR_{12}(19)$ A'3 $^QR_{23}(5)$, $^OP_{21}(5)$ $^OP_{12}(17)$, $^PQ13(17)$ A'3
$^QQ_{22}(9)$, $^SR_{21}(13)$ $^QR_{23}(7)$, $^OP_{21}(7)$ $^SR_{21}(15)$, $^RR_{12}(11)$ A'3
$^QQ_{22}(11)$, $^RQ_{11}(11)$ A'3 $^QR_{23}(9)$, $^OP_{21}(9)$
$^QR_{12}(5)$, $^OP_{12}(3)$, $^OP_{23}(3)$, $^SR_{21}(19)$ A'3 $^OP_{21}(11)$, $^QQ_{12}(9)$ A'3

3-0 Band

N	$^QQ_{11}$	$^QQ_{22}$	$^QQ_{33}$	$^QR_{12}$	$^QR_{23}$	$^OP_{21}$	$^OP_{32}$	$^OP_{12}$	$^OP_{23}$	$^SR_{21}$	$^SQ_{31}$
1	16.5*	6.6		13.1*	3.0*	8.2	2.1				0.7*
3	19.6*	3.3*	2.9	17.0	16.6*	12.8	9.2*	4.2*	1.7*		0.6*
5	24.7*	2.7*	5.2	21.8*	20.0*	19.7*	15.3	5.7	1.8*	1.2	0.4
7	29.6*	3.2*	5.4	25.3	23.6*	23.3*	19.4	4.8	1.9*	1.2*	
9	30.0*	3.3*	4.6	25.3	24.6*	24.4*	18.1*	4.0	1.9	1.2	
11	27.1	3.5*	3.5	21.6	22.3*	22.2*	17.9	3.0	1.6	1.3	
13	23.8	3.5*	2.5	18.1	16.3	16.8	15.2*	2.4	1.3	1.1	
15	19.6	2.9	1.3	13.3	12.8	13.5	12.3	1.6	1.1	0.8*	
17	14.9	2.3	0.8	9.4	9.3	9.0	8.4	1.0	1.0*	0.7	
19	10.1	1.9		6.2	5.9	6.2	5.8	0.6	0.4	0.5	
21	6.7	1.4		3.8	3.7	3.7	3.5	0.3			
23	4.2	0.8		2.5	2.2	2.0	2.0				
25	2.3	0.6		1.0	1.2	1.0	1.0				
27	1.1			0.6	0.2*	0.6	0.5*				
29	0.6										

$^QQ_{11}(1)$, $^QR_{23}(1)$ $^QQ_{22}(13)$, $^PQ(19)$ c7 $^QR_{23}(27)$, $^QQ_{32}(5)$ A'3
$^QQ_{11}(3)$, $^SR_{21}(7)$ $^QQ_{22}(17)$, $^QP_{11}(15)$ A'4 $^OP_{32}(13)$, $^RR_{(21)}$ c7
$^QQ_{11}(5)$, $^PQ_{23}(13)$ A'4 $^QR_{12}(1)$, $^QP_{32}(3)$ $^OP_{32}(27)$, $^PP_{33}(3)$ A'3
$^QQ_{11}(7)$, $^QQ_{22}(15)$ A'4 $^QR_{12}(5)$, $^PP_{22}(13)$ A'4 $^OP_{12}(3)$, $^OP_{23}(3)$
$^QQ_{11}(9)$, $^OP_{32}(9)$ $^QR_{23}(3)$, $^QP_{31}(21)$ A'4 $^OP_{12}(17)$, $^RR_{12}(19)$ A'4
$^QQ_{22}(3)$, $^PQ(15)$ c7, $^QQ_{32}(21)$ A'4 $^QR_{23}(5)$, $^QP_{21}(5)$ $^SR_{21}(15)$, $^SR_{21}(21)$ A'4
$^QQ_{22}(5)$, $^RQ_{31}(23)$ A'4 $^QR_{23}(7)$, $^QP_{21}(7)$, $^OP_{23}(5)$ $^SQ_{31}(1)$, $^SQ_{31}(3)$
$^QQ_{22}(9)$, $^OP_{23}(7)$ $^QR_{23}(9)$, $^QP_{21}(9)$
$^QQ_{22}(11)$, $^RR_{22}(19)$ A'4 $^QR_{23}(11)$, $^QP_{21}(11)$, $^RQ_{21}(19)$ A'4

Note. The values marked with an asterisk correspond to blended lines indicated at the bottom of the listing for each band. The missing values, (—), in the $(8–0)$, $(9–0)$, and $(10–0)$ bands denote saturated lines (see text). In the $(11–0)$ band, the cross sections of extra lines (with "e" superscript in the table) arising from interactions of the $A^3\Sigma_u^+$, $v = 11$ level with a $^3\Pi_u$ state are also given (see text and Ref. *(13)*).

TABLE 1a—*Continued*

4-0 Band

N	$^QQ_{11}$	$^QQ_{22}$	$^QQ_{33}$	$^QR_{12}$	$^QR_{23}$	$^QP_{21}$	$^QP_{32}$	$^OP_{12}$	$^OP_{23}$	$^SR_{21}$	$^SQ_{31}$
1	36.0	14.1		16.3	1.1*	9.7*	6.9			1.7	1.4
3	42.8*	7.2	4.5*	38.1	37.0*	33.6*	25.0*	11.1*	2.8*	3.5*	1.0*
5	56.5	7.3*	10.0	50.4	47.8*	47.4*	35.2	12.8	3.7	3.5*	1.0*
7	64.9	7.5	10.5*	53.8	56.0*	55.8*	42.5*	12.0	3.9	4.1	0.7
9	67.0*	7.6*	10.0*	57.6	58.0*	58.0*	42.0*	8.6	3.8	3.0*	
11	62.2*	8.0	7.8	49.1	45.5	45.3	40.4	9.4	4.3	3.1	
13	51.9*	8.5	4.2	41.5	35.6	33.9	32.5	5.5	3.1	2.4	
15	45.8*	7.0	3.6*	31.7*	30.1	31.5	31.8	3.9*	2.7	2.2	
17	33.9	5.8	2.4	22.5	21.2*	22.1	20.8	2.8	1.8	1.3	
19	23.5*	4.8	0.6	14.8	14.0	14.5	13.3	1.8	1.1*		
21	15.7	3.4		8.7	8.3	8.6	8.2	1.2	0.5		
23	9.5	2.1		5.0	4.8	4.8	5.0	1.5	0.6		
25	5.5	1.4		2.6	2.7	2.4	2.9				
27	2.9	0.6		1.1	1.1	1.2	1.1				
29	1.4			0.6	0.5	0.6					
31	0.3										

$^QQ_{11}(1)$, $^QQ_{33}(3)$, $^QR_{23}(1)$
$^QQ_{11}(3)$, $^PP_{22}(11)$ A'5
$^QQ_{11}(9)$, $^QP_{32}(9)$
$^QQ_{11}(11)$, $^PQ_{23}(15)$ A'5, $^SR_{11}(9)$ A'5
$^QQ_{11}(13)$, $^RQ_{21}(19)$ A'5
$^QQ_{11}(15)$, $^RQ(17)$ c8
$^QQ_{11}(19)$, $^SR_{11}(19)$ A'5
$^QQ_{22}(5)$, $^SR_{21}(9)$
$^QQ_{22}(9)$, $^RR_{32}(23)$ A'5

$^QQ_{33}(7)$, $^RR_{22}(15)$ A'5
$^QQ_{33}(9)$, $^OP_{33}(19)$ A'5
$^QQ_{33}(15)$, $^QQ_{22}(19)$ A'5
$^QR_{12}(15)$, $^RR(17)$ c8
$^QR_{23}(3)$, $^QP_{21}(3)$, $^PP(7)$ c8
$^QR_{23}(5)$, $^QP_{21}(5)$
$^QR_{23}(7)$, $^QP_{21}(7)$
$^QR_{23}(9)$, $^QP_{21}(9)$
$^QR_{23}(17)$, $^SR_{11}(17)$ A'5

$^OP_{21}(1)$, $^QP_{32}(3)$
$^QP_{32}(7)$, $^RQ(11)$ c8
$^OP_{12}(3)$, $^OP_{23}(3)$, $^QP_{21}(13)$ A'5
$^OP_{12}(15)$, $^QQ_{22}(21)$ A'5
$^OP_{23}(19)$, $^QP_{11}(19)$ A'5
$^SR_{21}(5)$, $^OP_{33}(17)$ A'5
$^SQ_{31}(5)$, $^QQ_{11}(31)$ A5

5-0 Band

N	$^QQ_{11}$	$^QQ_{22}$	$^QQ_{33}$	$^QR_{12}$	$^QR_{23}$	$^QP_{21}$	$^QP_{32}$	$^OP_{12}$	$^OP_{23}$	$^SR_{21}$	$^SQ_{31}$
1	62.5*	27.3		30.0*	10.0*	25.0*	12.4*			1.5*	3.5*
3	88.9	14.5	11.1	78.6	74.0*	67.8*	39.1	30.0*	10.0*	3.9	3.8
5	109	14.7*	22.2	113	93.7*	93.0*	73.1	26.1	9.0*	6.2	3.7*
7	131	14.7	23.5	113*	106*	106*	89.2	24.1	9.7	6.0	1.1
9	136	15.7	22.2	114	110*	110*	90.0*	19.7*	6.9	6.2	
11	128	17.0	16.6	103	102*	102*	85.8*	17.0*	6.8*	6.7	
13	109	15.6*	10.7	85.5	82.8*	83.2*	74.9	12.1	6.6	6.1	
15	91.2	14.5	6.7	62.5	60.4	61.0*	57.0	6.6	5.5	3.9	
17	68.3	14.0*	3.0	42.9	40.4	43.1	39.4*	5.5*	3.8	3.0	
19	50.3*	9.8	2.0	28.3	26.9	27.4	25.9	3.3	2.0	2.0	
21	30.4	7.0		16.8	16.8	17.1	16.2	2.1	0.9	0.9	
23	18.9	3.9		10.1	9.4	9.5	9.7	1.0	0.7	0.6	
25	10.6	2.6		5.0	5.0	5.2	5.0				
27	5.9	1.2		3.2	2.5	3.5	2.8				
29	2.5	1.0		1.2	0.9	1.0	1.1				
31	1.2*										

$^QQ_{11}(1)$, $^QR_{23}(1)$
$^QQ_{11}(5)$, $^OP_{12}(3)$, $^OP_{23}(3)$
$^QQ_{11}(9)$, $^QP_{32}(9)$
$^QQ_{11}(13)$, $^QQ_{12}(7)$ A'6
$^QQ_{11}(19)$, $^PP(13)$ c9
$^QQ_{11}(31)$, $^SQ_{31}(5)$ A4
$^QQ_{22}(5)$, $^OP_{31}(19)$ A'6, $^RR_{22}(13)$ A'6
$^QQ_{22}(13)$, $^OP_{23}(11)$, $^RR_{12}(9)$ A'6
$^QQ_{22}(17)$, $^RQ(13)$ c9
$^QR_{12}(1)$, $^QP_{21}(1)$, $^RR_{(23)}$ c10

$^QR_{12}(5)$, $^SQ_{31}(9)$
$^QR_{12}(7)$, $^OP_{23}(5)$
$^QR_{23}(3)$, $^QP_{21}(3)$
$^QR_{23}(5)$, $^QP_{21}(5)$, $^RQ_{21}(13)$ A'6
$^QR_{23}(7)$, $^QP_{21}(7)$
$^QR_{23}(9)$, $^QP_{21}(9)$
$^QR_{23}(11)$, $^QP_{21}(11)$
$^QR_{23}(13)$, $^PP(5)$ c9, $^RQ_{11}(9)$ A'6
$^QP_{21}(13)$, $^OP_{12}(11)$
$^QP_{21}(15)$, $^SR_{21}(21)$ A'6

$^QP_{32}(1)$, $^SR_{21}(1)$
$^QP_{32}(11)$, $^RP_{33}(19)$ A'6
$^QP_{32}(17)$, $^RR_{22}(21)$ A'6
$^OP_{12}(3)$, $^OP_{23}(3)$
$^OP_{12}(9)$, $^RQ_{11}(5)$ A'6
$^OP_{12}(17)$, $^RQ_{11}(17)$ A'6
$^SQ_{31}(1)$, $^QP_{21}(29)$ A6
$^SQ_{31}(5)$, $^RR_{22}(11)$ A'6

6-0 Band

N	$^QQ_{11}$	$^QQ_{22}$	$^QQ_{33}$	$^QR_{12}$	$^QR_{23}$	$^QP_{21}$	$^QP_{32}$	$^OP_{12}$	$^OP_{23}$	$^SR_{21}$	$^SQ_{31}$
1	110*	48.7		55.8*	15.0	51.3*	18.0*			5.3*	6.1
3	149	25.3	21.2	124*	120	107	73.2	36.0*	10.5*	8.0*	5.2*
5	184	23.0	36.0	170	151*	151*	120	37.5	15.3	11.0*	3.6
7	215	26.6	38.9	200	190*	189*	141	35.2	18.9	11.5*	
9	247*	26.1*	34.3	189	190*	190*	146*	31.8	13.4	12.8	2.7*
11	192	26.2*	26.8	153	155*	137*	139	24.8	13.0	10.6	2.3
13	174	27.0*	16.5*	137	126	127	139	18.7	10.7	9.0	
15	147	23.3	9.6	104	102	93.6	89.4	13.4*	8.5*	6.2	
17	119*	18.8	4.9*	71.2	68.0	67.9	65.0	8.5	6.0*	4.4	
19	76.5	14.3*	2.8*	44.5	45.5	45.4	43.3	6.0*	3.5	2.7	
21	49.4*	10.2		25.0*	25.3*	28.6	26.6	4.2*	2.1	1.7	
23	30.5	6.5*		16.1	16.1	15.2	15.3	2.1	1.0		
25	18.9	4.2		8.7	10.1	9.0	8.4	1.0*			
27	9.2	2.0*		5.1	5.0	4.4	4.6				
29	5.3			2.1	1.9	2.0*	2.6				
31	3.2			0.9		0.8	1.2				

$^QQ_{11}(1)$, $^QR_{23}(1)$, $^SR_{21}(5)$
$^QQ_{11}(9)$, $^QP_{32}(9)$
$^QQ_{11}(17)$, $^RR_{12}(13)$ A'7
$^QQ_{11}(21)$, $^QP_{11}(17)$ A'7
$^QQ_{22}(9)$, $^RR_{12}(29)$ A7
$^QQ_{22}(11)$, $^PQ_{23}(13)$ A7
$^QQ_{22}(13)$, $^SR_{11}(9)$ A'7
$^QQ_{22}(19)$, $^OP_{23}(17)$
$^QQ_{22}(23)$, $^SR_{11}(5)$ A'6
$^QQ_{22}(27)$, $^OP_{12}(25)$

$^QQ_{33}(13)$, $^OP_{33}(19)$ A'7
$^QQ_{33}(19)$, $^SR_{11}(17)$ A'7
$^QR_{12}(1)$, $^QP_{21}(1)$
$^QR_{12}(3)$, $^QP_{21}(19)$ A'7
$^QR_{12}(21)$, $^QQ_{12}(17)$ A'7
$^QR_{23}(5)$, $^QP_{21}(5)$
$^QR_{23}(7)$, $^QP_{21}(7)$
$^QR_{23}(9)$, $^QP_{21}(9)$, $^QQ_{11}(29)$ A7
$^QR_{23}(11)$, $^QP_{21}(11)$, $^PQ_{33}(19)$ A'7
$^QR_{23}(21)$, $^QP_{21}(19)$

$^OP_{21}(29)$, $^SQ_{31}(1)$ A5
$^QP_{32}(1)$, $^SR_{21}(1)$
$^OP_{12}(3)$, $^OP_{23}(3)$
$^OP_{12}(15)$, $^PP_{12}(11)$ A'7
$^OP_{12}(21)$, $^RQ(15)$ c10
$^OP_{23}(15)$, $^QP_{21}(19)$ A'7
$^SR_{21}(3)$, $^RR_{22}(9)$ A'7
$^SR_{21}(7)$, $^QQ_{32}(17)$ A'7
$^SQ_{31}(3)$, $^PQ_{33}(15)$ A'7
$^SQ_{31}(9)$, $^PQ_{23}(9)$ A'7

TABLE 1a—*Continued*

7-0 Band

N	$^QQ_{11}$	$^QQ_{22}$	$^QQ_{33}$	$^QR_{12}$	$^QR_{23}$	$^QP_{21}$	$^QP_{32}$	$^OP_{12}$	$^OP_{23}$	$^SR_{21}$	$^SQ_{31}$
1	140*	73.6*		78.5*	23.0*	73.0*	29.0*	60.0*	11.0*	4.7	10.5*
3	202	38.2	33.2*	182*	160	164	96.4*	60.0*		10.3*	11.6
5	267	34.7	48.8	241	239*	238*	166*	69.4	19.9	14.9*	10.0*
7	313	38.9	56.9	268	255*	254*	200	59.7	20.1*	20.0*	8.5*
9	322*	40.2	49.3	272	260*	259*	204*	54.7	20.2*	18.9	5.5*
11	317	40.9	41.3	253	249*	247*	193*	41.9	17.2	16.7	2.3*
13	285*	42.0	27.1	208	188	190	172	28.8	14.0*	12.5	
15	212	35.9	14.3*	149*	138	140*	131	19.0*	9.6	12.8	
17	160	28.4*	8.0*	103	101	101	63.7*	11.9	8.5	7.3	
19	111	21.0	3.0	69.9	65.1	67.2	63.8	7.5	5.0*	4.6	
21	74.5	15.7		42.5*	41.1	42.2	38.4	4.4		2.3	
23	47.3	11.4		26.3	22.3	23.1	21.3			1.1	
25	24.9	5.6		14.8	12.2	12.9	12.8				
27	8.8	2.6*		4.5	5.2	7.4	8.1				
29	6.0*			3.0*	3.2	3.1	2.1				
31	3.0*			2.3	1.9						

$^QQ_{11}(1)$, $^QR_{23}(1)$
$^QQ_{11}(9)$, $^OP_{32}(9)$, $^OP_{23}(7)$
$^QQ_{11}(13)$, $^PP_{22}(13)$ A'8
$^QQ_{11}(29)$, $^QR_{23}(9)$ A6, $^QP_{21}(9)$ A6
$^QQ_{11}(31)$, $^SR_{11}(11)$ A'7
$^QQ_{22}(1)$, $^QQ_{32}(15)$ A'8
$^QQ_{22}(17)$, $^PQ_{23}(17)$ A'8
$^QQ_{22}(27)$, $^QQ_{22}(7)$ A'7
$^QQ_{33}(3)$, $^SQ_{23}(5)$ A'8
$^QQ_{33}(15)$, $^QQ_{32}(21)$ A'8
$^QQ_{33}(17)$, $^PQ(17)$ c12
$^QR_{12}(1)$, $^QP_{21}(1)$, $^SR_{21}(5)$, $^QP_{31}(15)$ A'8

$^QR_{12}(3)$, $^SQ_{31}(7)$
$^QR_{12}(15)$, $^PQ_{23}(15)$ A'8, $^RQ_{11}(9)$ A'8
$^QR_{12}(21)$, $^OP_{23}(19)$
$^QR_{12}(29)$, $^QQ_{23}(9)$ A6
$^QR_{23}(5)$, $^SP_{21}(5)$, $^PQ(9)$ c12
$^QR_{23}(7)$, $^QP_{21}(7)$
$^QR_{23}(9)$, $^QP_{21}(9)$
$^QR_{23}(11)$, $^QP_{21}(11)$
$^QP_{21}(5)$, $^PQ(9)$ c12
$^QP_{21}(15)$, $^RR_{12}(9)$ A'8
$^QP_{32}(1)$, $^QR_{23}(25)$ A8
$^QP_{32}(3)$, $^PP_{22}(5)$ A'8

$^QP_{32}(5)$, $^OP_{12}(3)$, $^OP_{23}(3)$
$^QP_{32}(11)$, $^OP_{23}(9)$
$^QP_{32}(17)$, $^PP(17)$ c12
$^OP_{12}(15)$, $^PQ(17)$ c12
$^OP_{23}(13)$, $^RQ(17)$ c12
$^SR_{21}(3)$, $^SQ_{31}(5)$, $^QQ_{22}(5)$ A'8
$^SR_{21}(5)$, $^QP_{31}(15)$ A'8
$^SR_{21}(7)$, $^QQ_{22}(7)$ A'8
$^SQ_{31}(1)$, $^RR_{22}(5)$ A'8
$^SQ_{31}(11)$, $^PQ_{23}(9)$ A'8

8-0 Band

N	$^QQ_{11}$	$^QQ_{22}$	$^QQ_{33}$	$^QR_{12}$	$^QR_{23}$	$^QP_{21}$	$^QP_{32}$	$^OP_{12}$	$^OP_{23}$	$^SR_{21}$	$^SQ_{31}$
1	(−)	93.2		76.8*	39.7*	70.5*	36.1*	71.3	13.7	4.4	15.6
3	(−)	57.7*	37.0*	(−)	(−)	(−)	127	82.0	24.8*	11.2	14.0
5	(−)	48.0*	67.6	(−)	(−)	(−)	(−)	74.5	25.1	14.3*	11.6
7	(−)	49.1*	70.6	(−)	(−)	(−)	(−)	65.7	25.7*	21.2	
9	(−)	53.8	65.0	(−)	(−)	(−)	(−)	53.4*	23.6	23.0*	
11	(−)	52.7*	52.0	(−)	(−)	(−)	(−)	39.0	18.8	19.0*	5.4
13	(−)	48.1*	31.9	(−)	(−)	(−)	(−)	30.4	12.9	16.0*	
15	(−)	44.5	18.1*	202	172	192	173	19.7*	8.3*	11.0*	
17	198	37.1	10.0	139*	129	138	113	10.2	5.9	7.9	
19	150*	27.8	7.0	83.8*	83.3	86.6	82.3	5.2	3.4	5.8	
21	97.0	19.9		55.7	50.4	51.8	47.4	3.0		3.3	
23	60.4	12.7		34.6*	27.6	29.3	29.1				
25	34.5	8.1		15.7	15.2*	14.2*	15.5				
27	19.7	4.4		8.7	7.2	8.1*	7.5				
29	10.6*			5.7*	3.0	2.5	2.7				
31	3.5										

$^QQ_{11}(19)$, $^QP_{11}(13)$ A'9
$^QQ_{11}(29)$, $^PP(15)$ c12
$^QQ_{22}(3)$, $^QQ_{33}(23)$ A9
$^QQ_{22}(5)$, $^RR_{32}(15)$ A'9
$^QQ_{22}(7)$, $^QQ_{22}(7)$ A'9
$^QQ_{22}(15)$, $^PQ(19)$ c14
$^QQ_{33}(3)$, $^QP_{11}(1)$ A'9
$^QQ_{33}(11)$, $^QP_{32}(25)$ A9, $^PQ(3)$ c13
$^QQ_{33}(15)$, $^RR_{12}(7)$ A'9
$^QR_{12}(1)$, $^QP_{21}(1)$

$^QR_{12}(17)$, $^RR_{12}(11)$ A'9
$^QR_{12}(19)$, $^QQ_{12}(13)$ A'9
$^QR_{12}(23)$, $^SR_{11}(13)$ A'8
$^QR_{12}(29)$, $^QP_{11}(7)$ A'8
$^QR_{23}(1)$, $^RR_{22}(1)$ A'9
$^QR_{23}(25)$, $^SP_{32}(1)$ A7
$^QP_{21}(27)_2$ $^RQ_{31}(19)$ A'8
$^QP_{32}(1)$, $^SR_{21}(1)$ A'9
$^OP_{12}(11)$, $^RR_{32}(19)$ A'9
$^OP_{12}(17)$, $^QR_{12}(29)$ A9

$^OP_{23}(5)$, $^OP_{33}(13)$ A'9
$^OP_{23}(9)$, $^QQ_{11}(25)$ A9
$^OP_{23}(17)$, $^QP_{21}(29)$ A9
$^SR_{21}(5)$, $^SR_{21}(5)$ A'9
$^SR_{21}(9)$, $^QP_{32}(7)$
$^SR_{21}(11)$, $^OP_{32}(9)$
$^SR_{21}(13)$, $^QQ_{11}(11)$, $^QP_{32}(11)$, $^PP(3)$ c13
$^SR_{21}(15)$, $^QP_{32}(15)$

9-0 Band

N	$^QQ_{11}$	$^QQ_{22}$	$^QQ_{33}$	$^QR_{12}$	$^QR_{23}$	$^QP_{21}$	$^QP_{32}$	$^OP_{12}$	$^OP_{23}$	$^SR_{21}$	$^SQ_{31}$
1	(−)	105		117	43.3	108*	49.0			4.8	19.4
3	(−)	54.8	47.5	(−)	(−)	(−)	124	90.6	16.0*	14.4	22.7
5	(−)	56.5	72.1*	(−)	(−)	(−)	(−)	115*	25.8	21.5	16.1
7	(−)	54.5	86.3*	(−)	(−)	(−)	(−)	100	34.1	24.4	14.4
9	(−)	58.0*	77.3*	(−)	(−)	(−)	(−)	87.0	35.6	20.0*	11.5
11	(−)	58.4	56.4	(−)	(−)	(−)	(−)	68.3*	28.8	18.0	6.8
13	(−)	58.0*	37.6	(−)	(−)	(−)	(−)	51.4	24.1	16.4*	
15	(−)	53.5*	23.6*	(−)	(−)	197	176	32.7	16.7	16.0*	
17	(−)	44.5	13.0	152	138	140*	129	25.0*	8.5	7.1	
19	155*	33.9*	5.2	97.8	88.5	96.5*	87.8	13.3	9.2*	6.9	
21	101	24.3	4.2	60.3	53.1	58.3	54.9	7.5	3.6	4.4	
23	67.5	12.0*	3.0*	34.5*	34.0*	34.3	31.1	4.2	2.3		
25	35.0*	6.0*	1.4	13.2	12.0	12.0	16.8*				
27	15.5			6.9		7.7	4.8*				
29	9.4			3.6*	3.7	5.1*	3.7				

$^QQ_{11}(19)$, $^PP(23)$ c16
$^QQ_{11}(25)$, $^OP_{23}(9)$ A8
$^QQ_{22}(9)$, $^PP(11)$ c15
$^QQ_{22}(13)$, $^RQ(15)$ c15
$^QQ_{22}(15)$, $^PQ_{23}(13)$ A'10
$^QQ_{22}(19)$, $^SR_{11}(7)$ A'9
$^QQ_{22}(23)$, $^QQ_{11}(5)$ A8
$^QQ_{22}(25)$, $^QR_{23}(11)$ A8, $^QP_{21}(11)$ A8
$^QQ_{33}(5)$, $^OP_{23}(3)$
$^QQ_{33}(7)$, $^QP_{21}(3)$ A'10
$^QQ_{33}(9)$, $^PQ_{13}(15)$ A'11

$^QQ_{33}(15)$, $^SR_{11}(7)$ A'10
$^QQ_{33}(23)$, $^QQ_{22}(3)$ A8
$^QR_{12}(1)$, $^QP_{21}(1)$
$^QR_{12}(23)$, $^PP_{22}(3)$ A'9
$^QR_{12}(29)$, $^QP_{12}(17)$ A8
$^QR_{23}(23)$, $^QP_{32}(5)$ A8
$^QP_{21}(17)$, $^PQ(17)$ c15
$^QP_{21}(19)$, $^RR_{32}(5)$ A'9
$^QP_{21}(29)$, $^OP_{23}(17)$ A8
$^QP_{32}(25)$, $^QQ_{33}(11)$ A8, $^PQ(3)$ c13
$^QP_{32}(27)$, $^PQ_{33}(19)$ A'9

$^OP_{12}(5)$, $^SR_{21}(5)$ A'10
$^OP_{12}(7)$, $^PP_{22}(5)$ A'10
$^OP_{12}(11)$, $^OP_{33}(15)$ A'10
$^OP_{12}(17)$, $^PP_{12}(11)$ A'10
$^OP_{23}(19)$, $^SR_{31}(11)$ A'9
$^SR_{21}(9)$, $^PP(17)$ c16
$^SR_{21}(11)$, $^QR_{23}(9)$, $^QP_{21}(9)$, $^PQ(11)$ c15
$^SR_{21}(13)$, $^QP_{11}(17)$ A'11
$^SR_{21}(15)$, $^QP_{31}(17)$ A'10

TABLE 1a—*Continued*

10-0 Band

N	$^QQ_{11}$	$^QQ_{22}$	$^QQ_{33}$	$^QR_{12}$	$^QR_{23}$	$^QP_{21}$	$^QP_{32}$	$^OP_{12}$	$^OP_{23}$	$^SR_{21}$	$^SQ_{31}$	$^SR_{32}$
1	178*	93.3*		125*	27.4*	91.0*	30.8*		12.5	10.0*	19.0*	24.2
3	(–)	48.3	40.7	(–)	(–)	(–)	122	96.7	12.5	13.0*	20.0*	0.0
5	(–)	52.9*	63.8	(–)	(–)	(–)	(–)	110	26.1	16.0*	20.0*	
7	(–)	53.8	83.5	(–)	(–)	(–)	(–)	108*	25.5	21.0*	20.7*	
9	(–)	54.3	69.9	(–)	(–)	(–)	(–)	95.6	31.3*	23.7	14.3	
11	(–)	55.4	51.5	(–)	(–)	(–)	(–)	74.3*	25.9*	25.0	8.9	
13	(–)	51.0*	34.8	(–)	(–)	(–)	(–)	50.7*	21.2	14.8		
15	(–)	44.8	21.7	(–)	(–)	(–)	(–)	40.6	19.4	11.5		
17	(–)	39.5	9.0*	142	120*	129	113	24.1	10.9	8.2		
19	150	30.5	7.0	92.6	83.4	85.4	65.8	13.4	5.8*	5.9		
21	96.7	16.5		50.9	52.3	52.0	46.5	5.5	4.4			
23	57.1	10.0		30.0	26.2	27.0*	23.7*					
25	31.7	6.7		14.7	14.2	13.0	11.9					

$^QQ_{11}(1)$, $^RQ_{31}(9)$ A'11
$^QQ_{22}(1)$, $^QP_{21}(13)$ A'12
$^QQ_{22}(5)$, $^SR_{21}(7)$
$^QQ_{22}(13)$, $^rQ(9)$ c16
$^QQ_{22}(23)$, $^QR_{12}(13)$ A9
$^QQ_{33}(17)$, $^QQ_{12}(9)$ A'11
$^QR_{12}(1)$, $^QP_{21}(1)$
$^QR_{23}(1)$, $^SR_{21}(3)$

$^QR_{23}(17)$, $^QP_{21}(15)$ A'11
$^QP_{21}(1)$, $^SQ_{31}(5)$
$^QP_{21}(23)$, $^QQ_{11}(13)$, $^QP_{32}(13)$ A9
$^QP_{32}(1)$, $^QQ_{22}(15)$ A11
$^QP_{32}(23)$, $^QP_{21}(11)$ A'10
$^OP_{12}(7)$, $^QP_{21}(15)$ A'12
$^OP_{12}(11)$, $^RQ(15)$ c17
$^OP_{12}(13)$, $^RQ_{31}(17)$ A'11

$^OP_{23}(9)$, $^RQ_{11}(13)$ A'12
$^OP_{23}(11)$, $^RR(15)$ c17
$^OP_{23}(19)$, $^OP_{33}(11)$ A'10
$^SR_{21}(5)$, $^QR_{23}(3)$, $^QP_{21}(3)$
$^SQ_{31}(1)$, $^QQ_{33}(15)$ A11
$^SQ_{31}(3)$, $^QQ_{11}(15)$ A11, $^RQ_{21}(13)$ A'12
$^SQ_{31}(7)$, $^OP_{12}(15)$ A11

11-0 Band

N	$^QQ_{11}$	$^QQ_{22}$	$^QQ_{33}$	$^QR_{12}$	$^QR_{23}$	$^QP_{21}$	$^QP_{32}$	$^OP_{12}$	$^OP_{23}$	$^SR_{21}$	$^SQ_{31}$	$^SR_{32}$
1	118	73.2		67.1	35.5	77.0	36.1				24.2	11.6
3	168	38.4	32.2	164	166	160*	79.0	88.3	7.3*	10.0*	30.2	10.0*
	5.3*e											
5		7.8e	48.5	5.5e	46.0*e	44.7*e	115	98.6	14.0*	14.5	0.0*e	5.4*
	239	27.6		243	186*	182*		5.0*			22.4	
7	255	34.4	3.6e	250	238*	237*	10.9*	12.3*	16.2	14.6*		
	14.0e			47.7	11.7e		154	96.8*				
9	230	30.5	43.2	211*	212*	208*	166	76.0*	17.7	13.0*	20.4	
	53.5*	5.9e		45.4*	34.0*e	33.5*e		4.0*e				
11	29.7*	6.8e	3.4e	24.7e	29.3e	36.6e	6.8*	56.0	12.8	10.5	15.6	
	202	27.0	33.8	193	179	166	147	8.2*	3.7*e			
	3.8*				4.0*e	4.0*e						
13	50.6*e	5.7e	20.0	33.0*e	27.1*	31.1*	104	8.1*e	6.5	5.0		
	144	23.5	0.0*e	116	127	123	6.7*e	40.0	10.9			
	13.6e			9.6e								
15	57.6	21.5	1.3*	45.9	66.1	53.1*	63.0	5.6*e	7.2			
	51.1*e	7.0*e	3.8*e	16.8*e	25.0*	20.6e	32.0*	24.1				
17								9.6	2.1*			

$^QQ_{11}(3)$, $^SR_{32}(5)$
$^QQ_{11}(11)$, $^QP_{32}(11)$
$^QQ_{11}(13)$, $^rQ(11)$ c18
$^QQ_{11}(15)$, $^SQ_{31}(3)$ A10, $^RQ_{21}(13)$ A'12
$^QQ_{22}(15)$, ?
$^QQ_{33}(13)$, $^QR_{23}(9)$ A'11
$^QQ_{33}(15)$, $^QQ_{32}(7)$ A'11
$^QQ_{33}(15)$, $^SQ_{31}(1)$ A10
$^QR_{12}(9)$, $^rP(7)$ c18
$^QR_{12}(13)$, $^rP(11)$ c18
$^QR_{12}(15)$, $^RR_{22}(13)$ A'12

$^QR_{23}(5)$, $^QP_{21}(5)$
$^QR_{23}(5)$, $^QP_{21}(5)$
$^QR_{23}(7)$, $^QP_{21}(7)$, $^rQ_{33}(9)$ A'12
$^QR_{23}(9)$, $^QP_{21}(9)$
$^QR_{23}(9)$, $^QP_{21}(9)$, $^SR_{21}(5)$ A'12
$^QR_{23}(11)$, $^QP_{21}(11)$
$^QP_{21}(3)$, $^QP_{31}(7)$ A'12
$^QP_{21}(15)$, $^rP(9)$ c17
$^QP_{32}(13)$, $^rP_{22}(9)$ A'12
$^QP_{12}(7)$, $^SR_{21}(9)$
$^OP_{12}(9)$, $^rP(7)$ c18

$^OP_{12}(11)$, $^rQ(3)$ c17
$^OP_{12}(13)$, $^rP_{22}(11)$ A'12
$^OP_{12}(15)$, $^SQ_{31}(7)$ A10
$^OP_{23}(3)$, $^RQ(7)$ c19
$^OP_{23}(5)$, $^SR_{21}(7)$
$^OP_{23}(11)$, $^RQ(3)$ c17, $^RQ_{21}(9)$ A'12
$^OP_{23}(17)$, $^RR_{22}(7)$ A'11
$^SR_{21}(3)$, $^SQ_{31}(5)$
$^SQ_{31}(5)$, $^RQ_{31}(7)$ A'12
$^SR_{32}(3)$, $^rQ(5)$ c19

EXPERIMENTAL CONDITIONS

The experimental conditions used to record the absorption spectra were given in Paper I and consist of the association of a 50-m base pathlength multiple reflection cell built at the Université de Reims (*25*) and the mobile Bruker 120M Fourier transform spectrometer of the Université Libre de Bruxelles. At ambient temperature, paths of 201.84, 402.08, and 602.32 m with O₂ pressures varying from 20 to 750 Torr have been used (see Table 1 of Paper I). The path (4 m) between the cell and the spectrometer was taken into account for the calculation of the column densities of the gas. The unapodized resolution of 0.12 cm⁻¹ (maximum optical path difference of 7.5 cm) was of the same order of magnitude as the total linewidth in the UV region (~0.12 cm⁻¹ with 375 Torr of oxygen; see Yoshino *et al.* (*10*)). The line positions, widths, and intensities were measured directly from the absorption spectra using the SPECTRA program written by Carleer (*26*), which assumes for each line a Voigt profile convoluted by the instrumental function.

The accuracy on the line positions corresponding to the averaged value obtained from spectra at different pressures was estimated to be 0.005 cm⁻¹. As shown in Fig. 1 of Paper I, the intensities of the lines show a dynamic range of 10³, the lines of the *A–X* system being the stronger ones. In our experimental conditions, some of the *A–X* lines were saturated when column densities higher than 0.7 × 10²³ molecules cm⁻² were used. In this case the measurements were limited to lines for which the optical depth was ≤1.5. The accuracy of an intensity measurement is strongly dependent on the signal-to-noise ratio and on the intensity of the line itself. Because in FTS spectroscopy the noise is uniformly spread over the entire spectral region seen by the detector, higher signal-to-noise ratios are observed at

TABLE 1b
Integrated Cross Sections of Lines in the c–X (v'–0) Bands of O_2

2-0 Band

N	^RR	^RQ	^PQ	^PP
3	0.1	0.2	0.1	0.2
5	0.2	0.3	0.1	0.3
7	0.2	0.3	0.2	0.3
9	0.2	0.3	0.2	0.3
11	0.2	0.3	0.2	0.2
13	0.1	0.2	0.1	0.2
15	0.1	0.2	0.1	0.1
17		0.1		

3-0 Band

N	^RR	^RQ	^PQ	^PP
1	0.2	0.4		0.2*
3	0.4	0.6	0.3	0.5
5	0.5	0.8*	0.5	0.7
7	0.6	0.9	0.7	0.8
9	0.6	1.0	0.6	0.8
11	0.5	0.8	0.5	0.7
13	0.4	0.7	0.4	0.6
15	0.3	0.5	0.3	0.4
17	0.2	0.4	0.2	0.3
19	0.2	0.3	0.2	0.2
21	0.1	0.2	0.1	0.2

$^RQ(5)$, $^QR_{23}(15)$ A0, $^QP_{21}(15)$ A0
$^PP(1)$, $^QR_{12}(15)$ A0

4-0 Band

N	^RR	^RQ	^PQ	^PP
1	0.3	0.9		0.8
3	1.0	1.4	0.8	1.3
5	1.3	1.7	1.2	1.7
7	1.6	2.2	1.4	1.9
9	1.6*	2.2	1.4	1.8
11	1.2	2.0	1.2	1.7
13	1.0	1.6*	1.0	1.4
15	0.8	1.2	0.7	1.0
17	0.5	0.9	0.4	0.7
19	0.4	0.7	0.3	0.6
21	0.3	0.3	0.2	0.2
23		0.2		

$^RR(9)$, $^QP_{21}(21)$ A1
$^RQ(13)$, $^QR_{12}(23)$ A1

5-0 Band

N	^RR	^RQ	^PQ	^PP
1	0.8	1.7		1.4
3	1.8	2.2*	1.6	2.4
5	2.5	3.7	2.3	3.2
7	2.9	4.2	2.5	3.6
9	3.0	3.9	2.5	3.4
11	2.4	3.6	2.3	3.1
13	2.0	3.0	1.8	2.6
15	1.3	2.2	1.3	1.7
17	0.9	1.6	0.8	1.4
19	0.7	1.1	0.5	0.9
21	0.4	0.8	0.3	0.5
23	0.2	0.5	0.2	0.3
25		0.3		

$^RQ(3)$, $^QR_{12}(23)$ A2

6-0 Band

N	^RR	^RQ	^PQ	^PP
1	1.1	2.7		2.1
3	2.9	4.8	2.4	4.0
5	4.1*	6.1	3.9*	5.4
7	4.7	6.6	4.3	5.9
9	4.8	6.8	4.1	5.9
11	4.2	6.3	3.6	5.0
13	3.4	5.2	2.9	4.2
15	2.5	3.8	2.1	3.3*
17	1.9*	3.0	1.5	2.4*
19	1.1	1.9	1.0	1.5
21	0.6	1.2	0.6	1.1
23	0.4	0.7		0.4

$^RR(5)$, $^SR_{31}(3)$ A'3
$^RR(17)$, $^RQ_{21}(3)$ A'3
$^PP(5)$, $^RQ_{31}(5)$ A'3
$^PP(17)$, $^SR_{21}(13)$ A'3

7-0 Band

N	^RR	^RQ	^PQ	^PP
1	1.6	4.0		3.3
3	4.5	6.9	3.7	6.0
5	6.2	9.0	5.4	7.7
7	7.4	10.8	6.7	8.7*
9	7.3	10.6	6.2	8.8*
11	6.4	9.9	5.5*	7.5
13	5.1	7.7	4.5	6.2
15	3.8	6.0	3.2*	4.8
17	2.6	3.9*	2.0*	3.4
19	1.6	3.0	1.2*	2.2*
21	1.0*	2.2	0.8	1.1
23	0.7*	1.1		0.6
25				0.3

$^RR(21)$, $^QP_{32}(13)$ A3
$^RR(23)$, $^SR_{11}(17)$ A'4
$^RQ(17)$, $^RR_{22}(15)$ A'4
$^RQ(11)$, $^PP_{22}(7)$ A'4
$^RQ(15)$, $^QQ_{22}(3)$ A3, $^QP_{32}(21)$ A'4
$^PQ(17)$, $^QQ_{12}(5)$ A'4
$^PQ(19)$, $^QQ_{22}(13)$ A3
$^PP(7)$, $^PP_{31}(15)$ A'4, $^SR_{21}(3)$ A'4
$^PP(9)$, $^PP_{13}(15)$ A'4, $^QP_{21}(5)$ A'4
$^PP(19)$, $^QP_{21}(19)$ A'4

8-0 Band

N	^RR	^RQ	^PQ	^PP
1	1.7*	5.2*		4.2
3	6.4*	10.3	5.4	8.3
5	9.1	12.1	7.9*	9.5
7	10.6	14.6	8.9	12.5*
9	9.4	14.8	9.4*	12.8
11	8.8*	12.6*	7.8	10.8
13	7.3	9.9	6.8	8.1
15	5.7	8.9	3.5	5.8
17	4.0*	6.4*	2.8	3.8
19	2.5	4.3	2.0*	2.9
21	1.8	2.9	1.0	2.0
23	0.9	1.5	0.4	1.0
25	0.6	0.9		0.6
27	0.5	0.7		
29		0.4		

$^RR(1)$, $^RQ(27)$ c9, $^PP(25)$ c9
$^RR(3)$, $^QQ_{22}(9)$ A'5
$^RR(11)$, $^PQ(9)$
$^RR(17)$, $^QR_{12}(15)$ A4
$^RQ(1)$, $^PQ(25)$ c9
$^RQ(11)$, $^QP_{32}(7)$ A4
$^RQ(17)$, $^QQ_{11}(15)$ A4
$^PQ(5)$, $^QP_{21}(11)$ A'5
$^PQ(19)$, $^QQ_{22}(23)$ A'5, $^QQ_{12}(17)$ A'5
$^PP(7)$, $^QR_{23}(3)$ A4, $^QP_{21}(3)$ A4

9-0 Band

N	^RR	^RQ	^PQ	^PP
1	3.4	6.0*		5.2*
3	7.6*	13.2	6.5	10.0*
5	12.1	15.7	11.3*	14.0*
7	12.0*	19.0*	12.8	16.6
9	12.3	19.5*	11.5	15.8
11	11.2	17.2	8.1	13.9
13	9.2	14.0*	7.7	10.7*
15	7.4	10.7	5.5	8.4*
17	4.8	8.0	4.0	6.2
19	3.4	5.1	2.0	4.1
21	1.8	3.6	1.6	2.5
23	1.3*	1.6	0.8	1.2
25	0.7	1.1*	0.4*	0.6*
27		0.5*		

$^RR(3)$, $^PP(1)$
$^RR(5)$, $^PP(3)$
$^RR(7)$, $^PP(5)$, $^QP_{21}(12)$ A5, $^OP_{12}(11)$ A5
$^RR(23)$, $^RQ_{31}(11)$ A'5
$^RQ(1)$, $^QR_{23}(11)$ A5, $^QP_{21}(11)$ A5
$^RQ(7)$, $^PQ(5)$
$^RQ(9)$, $^PQ(7)$
$^RQ(13)$, $^QQ_{22}(17)$ A5
$^RQ(27)$, $^PP(25)$, $^SR(1)$ c8
$^PQ(25)$, $^RQ(1)$ c8
$^PP(13)$, $^QQ_{11}(19)$ A5
$^PP(15)$, $^QP_{21}(23)$ A'6

10-0 Band

N	^RR	^RQ	^PQ	^PP
1	3.8	7.0		7.0
3	9.2	14.7	8.0	12.6
5	13.0	19.0	11.6	15.5
7	15.7	21.4*	13.1	18.0*
9	15.2	23.4*	12.9	18.4
11	13.3	19.6*	9.6	15.2*
13	10.9	16.2	8.0*	13.1
15	8.2	12.0*	6.2	9.7*
17	5.4	9.3	4.1	7.7
19	3.6	6.4	2.5	5.4
21	1.9	4.4*	1.7	3.4
23	1.1*	2.5	0.7	1.1
25	0.6	1.3		0.7

$^RR(23)$, $^QR_{12}(1)$, $^QP_{21}(1)$ A5
$^RQ(9)$, $^PP(7)$
$^RQ(11)$, $^SR_{11}(19)$ A'7
$^RQ(15)$, $^OP_{12}(21)$ A6
$^RQ(21)$, $^OP_{33}(13)$ A'6
$^PQ(13)$, $^SR_{31}(1)$ A'6, $^SR_{31}(3)$ A'6
$^PP(11)$, $^RR_{12}(19)$ A'7
$^PP(15)$, $^RQ_{31}(9)$ A'6

11-0 Band

N	^RR	^RQ	^PQ	^PP
1	3.8	9.7		7.3
3	11.2	16.7	9.3	14.3
5	15.4	23.5	14.1	19.5
7	17.7*	24.8	16.5	21.5
9	18.5	25.5	15.2	21.2
11	15.6	24.0	12.7	18.3
13	11.6	19.5	11.2*	15.7*
15	9.9	16.0	9.2	12.3
17	6.9	9.7	4.6	8.7
19	4.4	6.8	3.4	8.3
21	2.9	4.5*	1.9*	3.4
23	1.1	2.7	0.8*	1.4
25	1.0*	2.2*		
27		0.9		

$^RR(7)$, $^PQ_{13}(3)$ A'7, $^PQ_{13}(17)$ A'8
$^RR(25)$, $^QQ_{12}(15)$ A'7
$^RQ(21)$, $^QP_{31}(21)$ A'7
$^RQ(25)$, $^OP_{11}(15)$ A'7
$^RQ(13)$, $^RQ_{31}(15)$ A'7
$^PQ(21)$, $^PP_{12}(9)$ A'7
$^PQ(23)$, $^OP_{33}(23)$ A'7
$^PP(13)$, $^RR_{32}(15)$ A'7

12-0 Band

N	^RR	^RQ	^PQ	^PP
1	5.3	10.6		8.0*
3	14.3	17.5*	9.8	15.9
5	16.0	25.3	16.2	21.9
7	20.1	29.2	18.3	24.7
9	18.8	29.3*	17.0*	26.4
11	16.6	27.8	14.2	23.3*
13	14.3	21.9	11.9*	19.7
15	12.9	3.1*	9.0	16.0*
	1.9e	16.7		
17	7.4	13.4*	7.0*	25.0*
			5.9*e	2.8e
19	5.2	8.5	3.1*	5.4
21	3.1*	6.3*	2.0*	3.5
23	2.4*	3.3		2.0
25		2.0*		

$^RR(21)$, $^QQ_{12}(15)$ A'8
$^RR(23)$, $^PP_{12}(17)$ A'8
$^RQ(3)$, $^PP(1)$
$^RQ(9)$, $^OP_{33}(13)$ A'8
$^RQ(17)$, $^OP_{23}(13)$ A7
$^RQ(21)$, $^OP_{11}(15)$ A'8
$^RQ(25)$, $^QQ_{32}(11)$ A'7
$^PQ(9)$, $^QR_{23}(5)$ A7, $^QP_{21}(5)$ A7
$^PQ(13)$, $^QP_{31}(19)$ A'8
$^PQ(17)$, $^OP_{12}(15)$ A7
$^PQ(17)$, $^QQ_{33}(17)$ A7
$^PQ(21)$, $^SR_{31}(1)$ A'7
$^PP(11)$, $^SR_{21}(13)$ A'8
$^PP(15)$, $^QQ_{11}(29)$ A8
$^PP(17)$, $^QP_{32}(17)$ A7

Note. The values marked with an asterisk correspond to blended lines indicated at the bottom of the listing for each band. In the (12–0) band, a few extra lines (with "e" superscript in the table) arising from the $c^1\Sigma_u^-$, $v = 12$–$A^3\Sigma_u^+$, $v = 7$ interaction (see text and Ref. (*13*)) are also given.

TABLE 1b—*Continued*

13-0 Band

N	^RR	^RQ	^PQ	^PP
1	4.4	10.5		8.4*
3	10.4	17.2	11.0*	15.0*
5	15.4	23.8*	14.2	20.6
7	17.3	25.2*	16.0	22.5
9	17.0	25.5*	15.1	24.3
11	15.0	23.1	13.3*	20.5
13	12.2	20.3	13.0	16.0
15	9.8	15.1	10.3*	13.6
17	6.6*	10.5	6.2	9.4
19	4.8	6.9	4.3	6.8*
21	3.4*	5.0*		3.2
23	1.2*	1.9*		

$^RR(17)$, $^QP_{31}(1)$ A'8, $^SR_{11}(17)$ A'9
$^RR(21)$, $^QQ_{32}(13)$ A'8
$^RR(23)$, $^QQ_{23}(9)$ A'8
$^RQ(5)$, $^RR(19)$ c14, $^QQ_{32}(17)$ A'9
$^RQ(7)$, $^PP_{22}(11)$ A'9
$^RQ(9)$, $^SR_{11}(5)$ A'9
$^RQ(21)$, $^QP_{31}(13)$ A'8
$^RQ(23)$, $^QP_{21}(9)$ A'8
$^PQ(3)$, $^QQ_{33}(11)$ A8, $^QP_{32}(25)$ A9
$^PQ(11)$, $^PP_{22}(15)$ A'9
$^PQ(13)$, $^RQ_{31}(23)$ A'9
$^PQ(15)$, $^RR_{12}(15)$ A'9
$^PP(1)$, $^RQ_{21}(11)$ A'9
$^PP(3)$, $^QQ_{11}(11)$ A8, $^QP_{32}(11)$ A8, $^SR_{21}(13)$ A8
$^PP(19)$, $^PP_{11}(19)$ A'9

14-0 Band

N	^RR	^RQ	^PQ	^PP
1	4.3	10.5*		9.5
3	12.8*	16.8	11.1*	17.6
5	16.7	23.2	15.0	20.0*
7	18.6	28.6	16.0	22.3
9	19.0*	30.5	16.4*	22.5*
11	16.3	23.0	14.5*	18.5
13	15.7	19.6	11.0	16.3
15	11.1	16.1	10.0*	13.0
17	7.1	12.8	8.0	10.4*
19	5.6*	9.6	6.0*	5.4
21	4.3	5.7	3.1*	4.0
23	1.8	2.7	1.2*	

$^RR(3)$, $^PP(21)$ c16, $^QP_{21}(23)$ A'11
$^RR(9)$, $^QP_{11}(11)$ A'10
$^RR(19)$, $^RQ(5)$ c13
$^RQ(1)$, $^RQ_{11}(7)$ A'10
$^PQ(3)$, $^QQ_{32}(19)$ A'10
$^PQ(9)$, $^QP_{31}(1)$ A'9
$^PQ(11)$, $^OP_{33}(21)$ A'10
$^PQ(15)$, $^QQ_{11}(3)$ A8
$^PQ(19)$, $^QQ_{22}(3)$ A8
$^PQ(23)$, $^PP_{12}(13)$ A'9
$^PP(5)$, $^SR_{21}(17)$ A'10
$^PP(9)$, $^RQ_{31}(3)$ A'9, $^QQ_{32}(1)$ A'9
$^PP(17)$, $^QQ_{22}(9)$ A'9

15-0 Band

N	^RR	^RQ	^PQ	^PP
1	4.3	10.3		10.2*
3	9.8	16.7	10.6	16.0
5	18.0*	24.7	13.8	19.6
7	18.2*	30.8*	16.9	22.0
9	18.7*	30.7*	19.0	23.1
11	15.1	23.9	13.0*	20.1*
13	13.8	22.1	10.4	18.4
15	10.3	18.0*	8.4*	13.7
17	7.9	10.2	5.9*	9.3*
19	4.8	8.8	3.0*	6.2*
21	2.4	4.9		4.7

$^RR(5)$, $^RR_{32}(9)$ A'10, $^OP_{33}(7)$ A'10
$^RR(7)$, $^PQ_{33}(9)$ A'10, $^RR_{12}(13)$ A'11
$^RR(9)$, $^RR(17)$ c16
$^RQ(7)$, $^RQ_{11}(13)$ A'11
$^RQ(9)$, $^RQ(17)$ c16
$^RQ(15)$, $^QQ_{22}(13)$ A9
$^PQ(11)$, $^QR_{23}(9)$ A9, $^QP_{21}(9)$ A9
$^PQ(15)$, $^QQ_{22}(13)$ A'10
$^PQ(17)$, $^QP_{21}(17)$ A9
$^PQ(19)$, $^PQ_{33}(5)$ A'9, $^RR_{22}(19)$ A'10
$^PP(1)$, $^RR_{12}(11)$ A'11
$^PP(11)$, $^QQ_{22}(9)$ A9
$^PP(17)$, $^PP_{22}(15)$ A'10
$^PP(19)$, $^RQ_{31}(7)$ A'9

16-0 Band

N	^RR	^RQ	^PQ	^PP
1	5.5	7.5		5.5*
3	7.6	14.5	7.5*	12.0*
5	13.9	18.0	10.7	16.0*
7	14.5*	21.0*	13.3	18.9
9	15.7	22.5	15.0*	19.7*
11	11.3	18.8	10.5*	16.5*
13	10.4	15.7	8.9	13.1
15	7.9	11.8	6.1	9.2
17	6.5*	8.0*	4.0	7.4*
19	3.2*	5.0	2.8	4.8
21	0.9	2.4		2.0*
23		1.2*		1.0*

$^RR(7)$, $^RQ_{12}(11)$ A10
$^RR(17)$, $^RR(9)$ c15
$^RR(19)$, $^RQ_{11}(17)$ A'11
$^RQ(7)$, $^QQ_{11}(11)$ A10
$^RQ(17)$, $^RQ(9)$ c15
$^RQ(23)$, $^RQ_{21}(17)$ A'10
$^PQ(3)$, $^QR_{12}(9)$ A10
$^PQ(9)$, $^QQ_{22}(13)$ A10
$^PQ(11)$, $^QQ_{11}(15)$ A10
$^PP(1)$, $^PQ(17)$ c18, $^PP(15)$ c18, $^QQ_{12}(11)$ A'12
$^PP(3)$, $^QR_{23}(9)$ A10, $^QP_{21}(9)$ A10, $^RQ_{31}(13)$ A'11
$^PP(5)$, $^PQ(13)$ c17
$^PP(9)$, $^PQ(15)$ c17
$^PP(11)$, $^QR_{12}(15)$ A10, $^QP_{31}(17)$ A'11
$^PP(17)$, $^SR_{21}(9)$ A9
$^PP(21)$, $^RR(3)$ c14, $^QP_{21}(23)$ A'11
$^PP(23)$, $^QQ_{11}(19)$ A9

17-0 Band

N	^RR	^RQ	^PQ	^PP
1	3.1	6.6*		6.2
3	7.8	11.5*	6.7*	10.7
5	10.1	15.5	8.5	12.0
7	12.8	17.4	11.2	15.1
9	12.4	18.8	11.7*	15.0*
11	11.0	16.0*	10.4	12.6
13	8.0*	14.2	8.0*	9.1
15	5.0*	11.0*	4.5*	8.2
17	3.6	8.8*	2.9	5.9
19			3.1	4.1

$^RR(13)$, $^QR_{23}(9)$ A10, $^QP_{21}(9)$ A10
$^RR(15)$, $^OP_{23}(11)$ A10
$^RQ(3)$, $^QP_{23}(11)$ A11, $^RQ_{21}(9)$ A'12
$^RQ(11)$, $^QR_{12}(5)$ A10
$^RQ(15)$, $^OP_{12}(11)$ A10
$^RQ(17)$, $^SR_{11}(7)$ A'11
$^PQ(3)$, $^OP_{12}(11)$ A11
$^PQ(9)$, $^OP_{33}(7)$ A'11
$^PQ(13)$, $^PP(5)$ c16
$^PQ(15)$, $^PP(9)$ c16
$^PP(9)$, $^QP_{21}(15)$ A11

18-0 Band

N	^RR	^RQ	^PQ	^PP
1	2.6	5.0*		2.6
3	5.5*	8.6	5.3	5.6
5	7.6	9.9	6.8*	10.0*
7	8.2	10.8	7.0*	10.0*
9	9.0	11.5	5.6	7.9
11	6.6	9.0	5.2*	7.0*
13	6.4	8.4	4.8	6.0
15			4.0*	5.8*
17			0.0*	0.0*

$^RR(3)$, $^QR_{23}(5)$ A11, $^QP_{21}(5)$ A11, $^QR_{12}(5)$ A11
$^RQ(1)$, $^PP_{32}(5)$ A11, $^PQ(33)$ A'12
$^PQ(5)$, $^QR_{23}(7)$ A11, $^QP_{21}(7)$ A11
$^PQ(7)$, $^QR_{12}(9)$ A11
$^PQ(11)$, $^QQ_{11}(13)$ A11
$^PQ(15)$, $^PP_{32}(11)$ A'11
$^PQ(17)$, $^PP(15)$, $^PP(1)$ c16, $^QQ_{12}(11)$ A'12
$^PP(5)$, $^QQ_{22}(7)$ A11
$^PP(7)$, $^OP_{12}(9)$ A11
$^PP(11)$, $^QR_{12}(13)$ A11

19-0 Band

N	^RR	^RQ	^PQ	^PP
1	3.9	3.5		
3	4.4	6.3	6.2	6.8*
5	3.8	5.8*	5.7*	6.5
7	3.0	6.0*	5.2*	6.2
9		4.0		7.1

$^RQ(5)$, $^QP_{31}(5)$ A'12
$^RQ(7)$, $^QP_{23}(3)$ A11
$^PQ(5)$, $^SR_{32}(3)$ A11
$^PQ(7)$, $^OP_{33}(7)$ A'12
$^PP(3)$, $^PQ_{33}(3)$ A'12

---

lower wavenumbers due to the higher emissivity of the Xe lamp source in this region. Estimating that the total uncertainty, including the uncertainties in the pressure, the temperature, and the path, is 3% for the strongest lines (integrated cross sections $\geq 10^{-24}$ cm^2 cm^{-1} molecule^{-1}), integrated line cross sections of 10^{-25} cm^2 cm^{-1} molecule^{-1} are measured with an uncertainty varying from 6% at 34 000 cm^{-1} to 20% at 41 000 cm^{-1}. Lines with integrated cross sections as low as 10^{-27} cm^2 cm^{-1} molecule^{-1} near 34 000 cm^{-1} and on the order of 10^{-26} cm^2 cm^{-1} molecule^{-1} near 41 000 cm^{-1} were measured with an uncertainty of about 30%. The integrated line cross-section values given in this work result from the average of at least three measurements made on spectra selected according to their signal-to-noise ratios and optical depth values.

RESULTS AND DISCUSSION

I. Integrated Line Cross Sections

Tables 1a, 1b, and 1c show the values of the integrated cross sections (in units of 10^{-26} cm^2 cm^{-1} molecule^{-1}) for the lines of the $A–X$, $c–X$, and $A'–X$ bands having $v' = $ 0–11, 2–19, and 2–12, respectively. The results of the (12–0) band analyzed in Paper I are not presented here because the lines are too weak to obtain reasonable values. The intensity for some of the Q form lines is not given for the (8–0), (9–0), and (10–0) bands of the $A–X$ system because these lines are saturated in our spectra. In Tables 1a, 1b, and 1c, the values marked by an asterisk correspond to blended lines. The intensity is then estimated from the

TABLE 1c
Integrated Cross Sections of Lines in the A'–X (v'–0) Bands of O$_2$

2-0 Band

Ω=1 sub-band

N	$^SR_{31}$	$^RR_{32}$	$^RQ_{31}$	$^QQ_{32}$	$^QP_{31}$	$^PQ_{33}$	$^OP_{33}$
1	0.2		0.3		0.2		
3	0.3		0.5		0.3	0.3*	
5	0.3	0.1	0.7	0.1*	0.4*	0.3	
7	0.4	0.2*	0.7*		0.4	0.3	
9	0.4*		0.7	0.2	0.5	0.2	
11	0.4	0.1	0.7	0.4	0.4	0.1	
13	0.3		0.6	0.2	0.5	0.1	0.1
15	0.3		0.4	0.2	0.3		
17	0.2		0.3*	0.2*	0.3*		
19	0.1*		0.3				
21			0.2				

Ω=2 sub-band

N	$^SR_{21}$	$^RR_{22}$	$^RQ_{21}$	$^QQ_{22}$	$^QP_{21}$	$^PQ_{23}$	$^PP_{22}$
1	0.2						
3	0.3	0.4	0.5	0.3	0.2		
5	0.4	0.4	0.5	0.5*	0.3*	0.2	0.1
7	0.6	0.3	0.7	0.5	0.4	0.1	0.2
9	0.5	0.3	0.8	0.6	0.4	0.1	0.2
11	0.5	0.3	0.8	0.4	0.4		0.1
13	0.4	0.2	0.8	0.4	0.3		
15	0.3	0.3	0.7	0.3	0.2		
17	0.3		0.6		0.2		
19	0.2		0.4				
21			0.2		0.1		
23			0.2				

$^SR_{31}(9), ^PQ_{33}(3)$ $^RQ_{31}(7), ^QP_{31}(5)$ $^QQ_{22}(5), ^QP_{21}(5)$
$^SR_{31}(19), ^RQ_{11}(17)$ $^QQ_{32}(17), ^QQ_{22}(5)$
$^RR_{32}(7), ^QQ_{32}(5)$ $^QP_{31}(17), ^QP_{21}(5)$

3-0 Band

Ω=1 sub-band

N	$^SR_{31}$	$^RR_{32}$	$^RQ_{31}$	$^QQ_{32}$	$^QP_{31}$	$^PQ_{33}$	$^OP_{33}$
1	0.5		0.8		0.3		
3	0.7*		1.3		0.8	0.5	0.1*
5	0.9		1.7*	0.3*	1.2	0.5	0.3
7	0.9		2.1	0.4*	1.6	0.7	0.2
9	0.9	0.3	2.0*	0.4*	1.5	0.6	
11	0.9	0.4	2.0	0.5	1.1	0.5	
13	0.6*	0.4	1.7	0.5	1.1	0.4	
15	0.5	0.4	1.2	0.4	0.7		
17	0.5	0.3	1.0	0.3	0.5		
19	0.3*	0.2	0.7		0.4		
21	0.3*		0.5		0.2		
23			0.3				

Ω=2 sub-band

N	$^SR_{21}$	$^RR_{22}$	$^RQ_{21}$	$^QQ_{22}$	$^QP_{21}$	$^PQ_{23}$	$^PP_{22}$
1	0.6	1.0	0.3	0.1*			
3	0.9	1.0	1.1*	1.0*	0.4*	0.3	
5	1.1*	1.1	1.5*	1.2	0.9	0.3	0.3
7	1.3*	0.9	2.0	1.4	0.9	0.2	0.4
9	1.4	0.8	2.3*	1.3	1.0	0.2	0.3
11	1.6	0.7	2.1	1.1	0.9		0.4
13	1.3*	0.6	2.4	0.8	0.9		0.3
15	1.0	0.3	1.8	0.6*	1.0		
17	0.7	0.2	1.5*	0.5	0.8		
19	0.5*		1.1	0.2	0.5		
21	0.4		0.9				
23			0.4				

Ω=3 sub-band

N	$^SR_{11}$	$^RR_{12}$	$^RQ_{11}$	$^QQ_{12}$	$^QP_{11}$	$^PQ_{13}$	$^PP_{12}$
7					0.2*		
9	0.2			0.2	0.4*		
11	0.2*	0.4*	0.4*	0.4*	0.2		0.1
13	0.3	0.4	0.2	0.3		0.2	0.2
15		0.3	0.3	0.4			0.3
17	0.2	0.4	0.2	0.4		0.3*	0.1
19		0.3*	0.3	0.3			
21		0.2	0.2	0.1			

$^SR_{31}(3), ^RR(5)$ c6 $^RQ_{31}(5), ^QP_{31}(3), ^PQ(5)$ c6 $^SR_{21}(7), ^QQ_{22}(1)$ $^RQ_{21}(3), ^RR(17)$ c6 $^SR_{11}(11), ^QQ_{12}(7)$ $^RQ_{11}(11), ^QQ_{22}(11)$ A2
$^SR_{31}(13), ^QQ_{32}(9)$ $^RQ_{31}(9), ^QQ_{32}(7)$ $^SR_{21}(13), ^PP(17)$ c6 $^RQ_{21}(5), ^QP_{21}(3)$ $^RR_{12}(11), ^SR_{11}(15)$ A2 $^QQ_{12}(11), ^QP_{32}(13)$ A2
$^SR_{31}(15), ^RQ_{31}(13)$ $^QQ_{32}(5), ^QR_{23}(27)$ A3 $^RR_{22}(5), ^QQ_{22}(3)$ $^RQ_{21}(17), ^QP_{12}(5)$ A2 $^RR_{12}(19), ^QR_{11}(19)$ A2 $^PQ_{13}(17), ^OP_{12}(17)$ A2
$^SR_{31}(19), ^SR_{21}(5)$ $^OP_{33}(3), ^PQ_{32}(27)$ A3 $^SR_{21}(19), ^QR_{12}(5)$ A2, $^OP_{12}(3)$ A2, $^OP_{23}(3)$ A2 $^QQ_{22}(15), ^QR_{23}(3)$ A2, $^QP_{21}(3)$ A2
$^SR_{31}(21), ^RQ_{21}(9)$ $^QQ_{22}(15), ^QR_{23}(3)$ A2, $^QP_{21}(3)$ A2

4-0 Band

Ω=1 sub-band

N	$^SR_{31}$	$^RR_{32}$	$^RQ_{31}$	$^QQ_{32}$	$^QP_{31}$	$^PQ_{33}$	$^OP_{33}$
1	1.2		2.1		0.4		
3	1.8		3.0		1.8	0.9	0.3
5	2.3	0.3	4.1		3.0*	1.5	0.4*
7	2.7	0.4	4.9	0.5	3.4*	1.6	0.6*
9	2.5*	0.6	5.5	0.8*	4.0	1.4*	0.6
11	2.1	0.6	4.4	1.0	2.7	1.1	0.5
13	1.8	0.6*	3.8	1.1	2.2	0.8	0.3*
15	1.2*	0.6	3.0*	1.0	1.7	0.5*	0.2*
17	1.1	0.5	2.1	0.7*	1.1	0.3	0.2
19	0.7	0.4	1.3*	0.6	0.8		
21	0.5*	0.3*	0.9	0.4*	0.6*		
23		0.2	0.5*		0.4		
25					0.0*		

Ω=2 sub-band

N	$^SR_{21}$	$^RR_{22}$	$^RQ_{21}$	$^QQ_{22}$	$^QP_{21}$	$^PQ_{23}$	$^PP_{22}$
1	1.3	1.9	0.7				
3	2.2*	2.3	2.2*	2.6	1.1		
5	2.7	2.4	3.4	3.3	1.6*	0.7	0.7
7	2.9	2.3	4.3	3.0	2.0*	0.5	0.6*
9	3.5	1.9	5.4	2.9	2.1	0.3	0.9
11	3.5*	1.6	5.3	2.5	2.2		0.9
13	3.1	1.3	4.4	1.9	1.6		0.8*
15	2.4*	1.0*	4.1	1.4*	1.7		0.6
17	1.7	0.5	3.3	0.8	1.3		
19	1.2	0.4*	2.4*	0.5	1.1*		
21	0.8*		1.8*	0.3	0.8		
23	0.6		0.8		0.4		
25			0.4				

Ω=3 sub-band

N	$^SR_{11}$	$^RR_{12}$	$^RQ_{11}$	$^QQ_{12}$	$^QP_{11}$	$^PQ_{13}$	$^PP_{12}$
7		0.6					
9		0.6		0.7	0.4		
11		0.7	0.6	0.9*	0.3		0.3
13	0.7	0.6	0.9*	1.0	0.3*	0.4	0.3
15	0.6	0.6	0.8	0.8	0.3*	0.4	0.3
17	0.4*	0.5	0.7	0.7			0.2
19	0.3	0.6*	0.6	0.6		0.5	
21		0.2	0.4	0.5			
23			0.3				

$^SR_{31}(9), ^QP_{31}(5)$ $^QQ_{32}(17), ^QP_{21}(7)$
$^SR_{31}(15), ^RR_{32}(13)$ $^QP_{31}(7), ^OP_{33}(5)$
$^SR_{31}(21), ^PP(29)$ c8 $^QP_{31}(15), ^SR_{21}(3), ^PP(7)$ c7
$^RR_{32}(21), ^SR_{21}(15)$ $^QP_{31}(21), ^QR_{23}$ A3
$^RQ_{31}(15), ^PP(27)$ c8 $^QP_{31}(25), ^QQ_{12}(11)$
$^RQ_{31}(19), ^OP_{33}(15)$ $^PQ_{33}(9), ^OP_{23}(25)$ A4
$^RQ_{31}(23), ^QQ_{22}(5)$ A3 $^PQ_{33}(15), ^QP_{21}(5), ^PP(9)$ c7
$^QQ_{32}(9), ^OP_{33}(7)$ $^OP_{33}(13), ^RQ_{21}(3)$
$^QQ_{32}(21), ^PQ(15)$ c7, $^QQ_{22}(3)$ A3

Note. The values marked with an asterisk correspond to blended lines indicated at the bottom of the listing for each band.

relative overall intensities of the bands and from the rotational distributions within the bands.

The only previous experimental values of integrated line cross sections are those of Yoshino *et al.* (*10*) for the *A–X* bands with $v' = 4$–11 and of Yoshino *et al.* (*21*) for the *c–X* bands with $v' = 6$–16. In the present work, in addition to the observation of other bands, the number of lines in each band has been extended (see Paper I); e.g., the integrated cross sections for the $^SQ_{31}$ lines are not mentioned by Yoshino *et al.*

(*10*) in the *A–X* bands, but are given for most of the bands in Table 1a.

For perturbed bands, the extra lines are indicated by "*e*" superscript in Tables 1a and 1b. To refer conveniently to the wavenumber listing given in Tables 1a and 1b of Paper I, the same listing order is adopted for the intensities. In agreement with theory, the extra lines borrow intensity from the more intense system that they perturb. Taking account of these extra lines is important, as illustrated in Fig. 1. This

TABLE 1c—*Continued*

5-0 Band

Ω=1 sub-band

N	$^SR_{31}$	$^RR_{32}$	$^RQ_{31}$	$^QQ_{32}$	$^QP_{31}$	$^PQ_{33}$	$^OP_{33}$
1	2.4		3.7		0.5		
3	3.4		5.4		3.3	2.3	
5	4.0		7.5		5.3	3.0	0.8
7	4.3	0.6	8.1	1.0	6.3	3.0*	1.3
9	4.0	1.1	9.6	1.5	6.4	2.7	1.3
11	4.2	1.2	7.6*	1.4	5.0	2.3	1.1
13	3.6	1.2	7.2	1.9	4.1	1.5	0.6
15	2.6	1.3	5.5	1.6	3.4	0.8	
17	1.8	1.0	4.2	1.5	1.9		
19	1.2*	0.7	2.3	1.3	1.3		0.1*
21	1.0*	0.3	0.8*	0.9	0.8		
23		0.1*		0.6	0.4*		
25				0.5*			

$^SR_{31}(19)$, $^QP_{21}(5)$
$^SR_{31}(21)$, $^RQ_{21}(11)$
$^RR_{32}(23)$, $^QQ_{22}(9)$ A4
$^RQ_{31}(11)$, $^RR(23)$ c9
$^RQ_{31}(21)$, $^PQ_{23}(11)$

$^QQ_{32}(23)$, $^RR_{12}(9)$
$^QQ_{32}(25)$, $^RR_{22}(21)$, $^PP_{12}(11)$
$^QP_{31}(23)$, $^RQ_{11}(9)$
$^PQ_{33}(7)$, $^QQ_{12}(23)$ A'6
$^OP_{33}(19)$, $^QQ_{33}(9)$ A4

Ω=2 sub-band

N	$^SR_{21}$	$^RR_{22}$	$^RQ_{21}$	$^QQ_{22}$	$^QP_{21}$	$^PQ_{23}$	$^PP_{22}$
1	2.9	3.7	1.2				
3	4.1	4.3	4.1	2.8	2.2	0.9	0.7
5	5.2	4.7	6.8	5.1	2.7*	1.4	1.1
7	5.8	4.7	8.3*	5.7	3.5	1.2	1.9
9	6.4*	3.5	9.6	6.1*	3.7	0.6	2.0
11	6.8	2.8	9.7*	4.5*	4.3	0.6*	1.7*
13	5.0	2.4	8.9	3.5	3.8*		1.6
15	4.5	2.0*	8.1	2.1	3.4	0.5*	1.4
17	3.4	1.2	6.2	1.9	2.9		1.2
19	2.3*	0.7*	4.4*	1.6*	2.4		
21	1.7	0.4*	3.3*	1.5	1.5		0.4
23	0.9		1.8	0.9*	1.3*		
25	0.8		1.1	0.3*	0.6		
27			0.5				

$^SR_{21}(9)$, $^RQ_{21}(7)$
$^SR_{21}(19)$, $^QP_{11}(5)$
$^SR_{21}(21)$, $^RQ_{11}(11)$
$^RR_{22}(15)$, $^QQ_{33}(7)$ A4
$^RR_{22}(21)$, $^QR_{12}(13)$ A4
$^RQ_{21}(19)$, $^QQ_{11}(13)$ A4
$^QQ_{22}(23)$, $^QQ_{12}(17)$, $^PQ(19)$ c8
$^QP_{21}(13)$, $^OP_{12}(3)$ A4, $^OP_{23}(13)$ A4
$^PQ_{23}(15)$, $^SR_{11}(9)$, $^QQ_{11}(11)$ A4

$^RQ_{21}(21)$, $^PQ_{13}(11)$
$^QQ_{22}(25)$, $^RR(3)$ c8
$^QQ_{22}(11)$, $^PP(5)$ c8
$^QQ_{22}(9)$, $^QQ_{33}(15)$ A4
$^QQ_{22}(21)$, $^OP_{12}(15)$ A4
$^QQ_{22}(25)$, $^RQ_{11}(21)$
$^PP_{21}(11)$, $^PP(5)$ c8
$^PP_{21}(23)$, $^QP_{11}(17)$
$^PP_{22}(11)$, $^QQ_{11}(3)$ A4

Ω=3 sub-band

N	$^SR_{11}$	$^RR_{12}$	$^RQ_{11}$	$^QQ_{12}$	$^QP_{11}$	$^PQ_{13}$	$^PP_{12}$
5	0.6				0.3*		
7	0.7			0.9	0.7		
9	0.8*	0.9*	1.5*	1.3			0.4
11	0.8	1.3	1.5*	1.6	0.8	0.8*	0.9*
13	1.2	1.2	1.4	1.9	0.8	0.9	0.7
15	1.1	1.1	1.5	2.0	0.7	0.7	0.8
17	1.0*	1.0	1.5	1.9*	0.5*	0.6	0.7
19	0.8*	0.9	1.1	1.3	0.4*	0.4	0.6
21	0.4	0.5	0.8*	1.1		0.3	0.5
23		0.2	0.6	0.7			

$^SR_{11}(17)$, $^QR_{23}(17)$ A4
$^SR_{11}(19)$, $^QQ_{11}(19)$ A4

$^QQ_{12}(17)$, $^PQ(19)$ c8
$^QP_{11}(19)$, $^OP_{23}(19)$ A4

6-0 Band

Ω=1 sub-band

N	$^SR_{31}$	$^RR_{32}$	$^RQ_{31}$	$^QQ_{32}$	$^QP_{31}$	$^PQ_{33}$	$^OP_{33}$
1	5.2*		5.5		1.7*		
3	6.2*	0.7	8.4*	0.3*	6.6	3.5	0.6
5	6.7*	1.0*	12.1*	0.8	8.2	4.8	1.3
7	7.9	1.6	15.0	1.4	9.3	5.0	2.0
9	8.0	1.8	14.6*	2.2	9.5	4.7	2.3
11	6.7	2.2	14.1	2.9	8.4	3.5	1.6
13	5.6	2.3	11.0	3.1	6.7	2.7*	1.4
15	4.8	1.9	9.3	2.7	4.9*	1.4	1.2
17	3.5*	1.6	5.5	2.4	3.8	0.8	1.1*
19	2.3	1.6	4.3	2.0	2.1*		0.6*
21	1.4	1.1*	3.1	1.9	1.6		
23		0.9	1.9	0.9	1.4		
25		0.4					

$^SR_{31}(1)$, $^SR_{31}(3)$, $^PQ(13)$ c10
$^SR_{31}(5)$, $^QQ_{22}(23)$ A6
$^SR_{31}(17)$, $^PQ_{13}(19)$, $^PP_{12}(23)$ A'7
$^RR_{32}(5)$, $^PQ_{13}(19)$ A'7
$^RR_{32}(21)$, $^QP_{21}(13)$
$^RQ_{31}(3)$, $^QP_{31}(1)$
$^RQ_{31}(5)$, $^QQ_{32}(3)$

$^RQ_{31}(9)$, $^PP(15)$ c10
$^QQ_{32}(15)$, $^RQ_{21}(5)$
$^QP_{31}(15)$, $^QP_{21}(3)$
$^QP_{31}(19)$, $^RR_{22}(13)$, $^QQ_{22}(5)$ A5
$^OP_{33}(13)$, $^RQ(21)$ c10
$^OP_{33}(17)$, $^QQ_{23}(11)$
$^OP_{33}(19)$, $^QP_{32}(11)$ A5

Ω=2 sub-band

N	$^SR_{21}$	$^RR_{22}$	$^RQ_{21}$	$^QQ_{22}$	$^QP_{21}$	$^PQ_{23}$	$^PP_{22}$
1	5.8*	6.4	2.8		1.3*		
3	7.8*	7.2	6.3*	4.2	3.8*	1.3	0.9
5	8.8	7.6	10.5*	8.8	5.2	2.4	2.1
7	9.6	7.6	15.1	9.7	5.7	1.3	2.7
9	11.1	6.2	16.3	9.7	6.2	1.3	3.0
11	10.7	4.6*	16.4	7.8	5.8	1.2*	3.1
13	8.9	3.9*	14.5*	6.1	5.9*	1.2	2.6*
15	7.3	2.5	12.3	3.9	5.9		1.6
17	5.4*	1.7	10.2	2.5	4.8		0.9
19	3.7	0.8	7.8	1.7*	3.6*		0.8
21	2.5*	0.6*	5.2	1.2	2.4		
23	1.5		3.2		1.5*		
25	0.9		2.1		0.7		
27			1.1				

$^SR_{21}(1)$, $^SR_{21}(3)$
$^SR_{21}(17)$, $^PP_{22}(13)$
$^SR_{21}(21)$, $^QP_{21}(15)$ A5
$^RR_{22}(11)$, $^SQ_{31}(5)$ A5
$^RR_{22}(21)$, $^QP_{32}(17)$ A5
$^RQ_{21}(13)$, $^QR_{23}(15)$ A5, $^QP_{21}(5)$ A5

$^RQ_{21}(3)$, $^QP_{21}(1)$
$^QQ_{22}(19)$, $^RR_{12}(13)$
$^QP_{21}(19)$, $^RQ_{11}(13)$
$^QP_{21}(23)$, $^PP(15)$ c9
$^PP_{22}(13)$, $^SR_{21}(17)$

Ω=3 sub-band

N	$^SR_{11}$	$^RR_{12}$	$^RQ_{11}$	$^QQ_{12}$	$^QP_{11}$	$^PQ_{13}$	$^PP_{12}$
5			0.3*	1.0			
7	1.1*	0.6*	1.1	1.3*			
9	1.4*	2.0*	1.0*	1.8	1.1		
11	1.7	2.3	1.8	3.1	1.2	1.1	1.3*
13	1.8	2.3*	2.2*	3.7	1.2	1.3	1.1
15	1.7	2.2	2.3	3.2	0.9	1.1	1.1
17	1.5	1.8	2.2*	2.7	1.0	0.8	1.0
19	1.2	1.4	2.0	2.2	1.0	0.8	0.6
21	0.7	0.8	1.0	1.8			
23			0.8	0.9*			
25					0.3		

$^SR_{11}(7)$, $^RQ_{11}(5)$, $^OP_{12}(9)$ A5
$^SR_{11}(9)$, $^RR_{12}(7)$
$^RQ_{11}(17)$, $^OP_{12}(17)$ A5
$^RR_{12}(9)$, $^QQ_{22}(13)$ A5, $^OP_{23}(11)$ A5
$^RQ_{11}(9)$, $^QR_{23}(13)$ A5, $^OP_{12}(11)$ A5

$^QQ_{12}(7)$, $^QQ_{11}(13)$ A5
$^QQ_{12}(23)$, $^PQ_{33}(7)$ A'5

7-0 Band

Ω=1 sub-band

N	$^SR_{31}$	$^RR_{32}$	$^RQ_{31}$	$^QQ_{32}$	$^QP_{31}$	$^PQ_{33}$	$^OP_{33}$
1	5.8*		7.4		2.3		
3	8.0		13.6		5.9	3.3*	
5	10.3		17.4	1.4*	10.0	5.4	
7	10.5	1.3	20.2	1.9	13.8	7.1	3.2
9	10.1	2.7	20.8	2.4	14.0	6.8	2.8
11	10.5	2.6	19.0	4.0*	11.6	4.0	2.2
13	7.5	2.6*	16.5	4.5	8.7	3.4	1.5
15	6.5	2.6*	13.2*	4.4	6.3	2.2*	1.0*
17	4.4	2.5	8.4	3.0*	4.7*	1.8	0.8*
19	3.4	1.7	6.2	2.4	4.5	1.0*	0.5*
21	2.3	1.2	4.3	2.0*	1.8*		
23	1.1	0.9	1.9	1.2	1.3		
25			0.8	1.2			

$^SR_{31}(1)$, $^PQ(21)$ c12
$^RR_{32}(13)$, $^QQ_{32}(21)$ A'8
$^RR_{32}(15)$, $^PP(13)$ c11
$^RQ_{31}(15)$, $^PQ(13)$ c11
$^QQ_{32}(5)$, $^QQ_{22}(23)$ A'8
$^QQ_{32}(11)$, $^RQ(25)$ c12
$^QQ_{32}(17)$, $^SR_{21}(7)$ A6
$^PQ_{33}(3)$, $^RQ_{11}(19)$ A'8, $^PQ_{13}(17)$ A'8, $^RR(7)$ c11
$^PQ_{33}(19)$, $^QR_{23}(11)$ A6, $^QP_{21}(11)$ A6

$^QQ_{32}(21)$, $^RR(21)$ c11
$^QP_{31}(17)$, $^OP_{33}(15)$
$^QP_{31}(21)$, $^RQ(21)$ c11
$^PQ_{33}(15)$, $^SQ_{31}(3)$ A6
$^OP_{33}(17)$, $^SR_{21}(15)$
$^OP_{33}(19)$, $^QQ_{33}(13)$ A6

Ω=2 sub-band

N	$^SR_{21}$	$^RR_{22}$	$^RQ_{21}$	$^QQ_{22}$	$^QP_{21}$	$^PQ_{23}$	$^PP_{22}$
1	6.1	9.3	3.2				
3	9.0	10.6	9.6	7.6	5.2	1.4	2.3
5	12.6	10.0	15.0	12.5	7.0	2.0*	2.7
7	13.7	11.2	20.1	14.0*	7.9	2.2	4.1
9	14.3	10.0	22.6	13.5	9.0*	3.3*	4.5
11	15.0	8.6	22.0	10.4	9.5	1.9	4.0
13	13.3	5.6	20.6	8.9	9.3	1.4*	3.6
15	10.3*	3.9	18.6	6.1	8.5	1.2	2.4
17	8.2	1.8	14.2	4.0	7.0	0.4	1.4
19	7.7	1.2	10.1	2.4	4.9*		1.1*
21	4.1	0.8	6.6		3.7		
23	2.7		4.9		2.1		
25	1.1		2.7		1.1		
27	0.6		1.1				
29			0.7				

$^RR_{22}(7)$, $^PQ_{23}(5)$
$^RR_{22}(9)$, $^SR_{21}(3)$ A6
$^QQ_{22}(7)$, $^QQ_{22}(27)$ A7
$^QP_{21}(9)$, $^QR_{12}(3)$ A6

$^QP_{21}(19)$, $^QP_{23}(15)$ A6
$^PQ_{23}(9)$, $^SQ_{31}(9)$ A6
$^PQ_{23}(13)$, $^QQ_{22}(11)$ A6
$^PP_{22}(19)$, $^RR_{12}(15)$

Ω=3 sub-band

N	$^SR_{11}$	$^RR_{12}$	$^RQ_{11}$	$^QQ_{12}$	$^QP_{11}$	$^PQ_{13}$	$^PP_{12}$
5		0.9	1.5				
7	1.4	1.4	2.1	2.0		0.6	
9	1.6*	2.5	3.2	3.0		1.0	0.8*
11	2.1*	3.5	3.8	3.9	1.6	1.5	1.0
13	2.4	3.0*	3.5	4.7	2.9	2.0	1.3
15	2.7	2.8*	3.5	4.5*	3.6*	1.8	1.8
17	1.4*	2.4	3.4	3.3	2.2*	1.3	1.7
19	1.0*	1.5*	2.1	3.0	1.0	0.6*	1.1
21			1.9		1.0		0.8
23					0.7		0.2*

$^SR_{11}(9)$, $^QQ_{22}(13)$ A6
$^SR_{11}(11)$, $^QQ_{11}(31)$ A7
$^SR_{11}(17)$, $^QQ_{33}(19)$ A6
$^SR_{11}(19)$, $^RQ(11)$ c10
$^RR_{12}(13)$, $^QQ_{11}(17)$ A6
$^RR_{12}(19)$, $^PP(11)$ c10
$^PP_{12}(23)$, $^SR_{31}(17)$ A6, $^PQ_{33}(13)$ A6

$^QQ_{12}(15)$, $^RR(25)$ c11
$^QP_{11}(15)$, $^RQ(25)$ c11
$^QP_{11}(17)$, $^QQ_{11}(21)$ A6
$^PQ_{13}(19)$, $^RR_{32}(5)$ A'6
$^PP_{12}(9)$, $^PQ(21)$ c11

figure presents the values of the integrated cross sections for the lines previously assigned (*1, 5, 7, 9*) in the $^QQ_{11}$, $^QR_{23}$, and $^QQ_{22}$ branches of the perturbed *A–X* (11–0) band and the values obtained by adding the integrated cross sections of extra lines newly observed and assigned to a new $^3\Pi_u$–$X^3\Sigma_g^-$ transition in Paper I. It can be seen that the contribu-

TABLE 1c—*Continued*

8-0 Band

Ω=1 sub-band

N	$^SR_{31}$	$^RR_{32}$	$^RQ_{31}$	$^QQ_{32}$	$^OP_{31}$	$^PQ_{33}$	$^OP_{33}$
1	8.2		9.8		4.0·		
3	11.4	1.5	16.4	1.6	9.8	5.2	1.5
5	13.3	1.8	21.4	2.1	15.1	8.0	3.2
7	13.7	2.1	25.0	2.8	17.9	8.6	5.0
9	13.9·	2.3	24.2	3.4	16.1	8.1	4.3
11	12.1	3.4	23.6	5.9	13.5	6.0	2.8
13	10.1·	3.2·	21.3	6.5	11.4·	4.8	2.3
15	8.1	3.0·	17.0	5.5	8.6·	4.5	1.8
17	5.9	2.5	11.6	4.7	6.5·	2.2	1.5
19	4.2	2.2	8.9·	4.2	4.8·		
21	2.8	1.7	5.6	3.0·	3.4		
23			3.0	1.8	1.6		
25			2.0		1.1		

$^SR_{31}(9)$, $^QQ_{22}(21)$ A'9
$^SR_{31}(13)$, $^QR_{12}(23)$ A8
$^RR_{32}(13)$, $^SR_{11}(21)$ A'9
$^RR_{32}(15)$, $^OP_{21}(3)$
$^RQ_{31}(19)$, $^QP_{21}(27)$ A8
$^QQ_{32}(13)$, $^RR(21)$ c13
$^OP_{31}(1)$, $^SR_{11}(17)$ A'9, $^RR(17)$ c13
$^OP_{31}(15)$, $^QR_{21}(1)$ A7, $^QP_{21}(1)$ A7, $^SR_{21}(5)$ A7

$^QQ_{32}(15)$, $^QQ_{22}(1)$ A7
$^QQ_{32}(17)$, $^RR_{22}(11)$
$^QQ_{32}(21)$, $^QQ_{33}(15)$ A7
$^OP_{31}(13)$, $^RQ(21)$ c13
$^OP_{31}(17)$, $^RQ_{21}(11)$
$^OP_{31}(19)$, $^RQ(13)$ c12
$^OP_{33}(13)$, $^RQ(9)$ c12

Ω=2 sub-band

N	$^SR_{21}$	$^RR_{22}$	$^RQ_{21}$	$^QQ_{22}$	$^OP_{21}$	$^PQ_{23}$	$^PP_{22}$
1	7.3	10.7	3.2				
3	12.0	12.7	11.6	10.5	5.5·	1.2	
5	16.0	14.5·	20.0	15.0·	8.4	2.0·	3.0·
7	19.4	15.3	24.8	20.6·	11.2	1.9	5.7
9	20.7	11.6	28.0	18.5·	11.8	1.3·	4.7
11	18.7	10.7·	30.3·	12.6	12.0	1.2	3.8
13	17.0·	8.9	27.3	11.6	10.8	1.1	3.2
15	13.5	5.9	23.1	7.9	10.3	1.1	2.8
17	10.2	5.7	16.4	5.8·	8.7	1.0·	2.2
19	7.1	3.6	11.7	3.8	5.9		1.6·
21	5.6	3.2·	8.3	1.4	3.8		1.3
23	3.3		5.8	1.3·	2.7		
25	2.0·		3.4		2.0		
27	1.0		1.3		1.2		

$^SR_{21}(3)$, $^PP_{12}(19)$ A'9
$^SR_{21}(13)$, $^PP(11)$ c12
$^SR_{21}(25)$, $^RR_{12}(19)$
$^RR_{22}(5)$, $^SQ_{11}(11)$ A7
$^RR_{22}(21)$, $^PP_{22}(19)$
$^QQ_{22}(7)$, $^SR_{21}(7)$ A7
$^QQ_{22}(5)$, $^SR_{21}(3)$ A7, $^SQ_{31}(5)$ A7

$^QQ_{22}(9)$, $^RR(23)$ c13
$^QQ_{22}(17)$, $^RQ_{11}(11)$
$^QQ_{22}(23)$, $^QQ_{32}(5)$ A'7
$^PQ_{23}(5)$, $^QQ_{33}(3)$ A7
$^PQ_{23}(9)$, $^SQ_{31}(11)$ A7
$^PQ_{23}(17)$, $^QQ_{22}(17)$ A7
$^PQ_{23}(15)$, $^RQ_{11}(9)$, $^QR_{12}(15)$ A7

Ω=3 sub-band

N	$^SR_{11}$	$^RR_{12}$	$^RQ_{11}$	$^QQ_{12}$	$^OP_{11}$	$^PQ_{13}$	$^PP_{12}$
3	0.8						
5	1.3·			1.5			
7	3.0	2.0	2.9	2.4	2.0·		
9	3.2	3.2·	3.7·	3.5	2.4		1.0·
11	2.9	4.2·	5.0·	4.1	2.8	1.0·	1.5·
13	3.1	4.1·	5.0·	5.7	2.1	1.7·	1.4
15	3.0	3.0·	4.5·	5.3·	1.8·	2.2·	1.4
17	2.8	2.0	4.0·	4.8	1.3	2.0·	1.6·
19	2.7	1.7·	2.8·	3.2	1.2	1.2	1.3
21		1.5	2.3	2.7·		1.0	1.1
23		0.9	1.5	1.8			

$^RR_{12}(9)$, $^QP_{21}(15)$ A7
$^RR_{12}(11)$, $^PP_{12}(9)$
$^RR_{12}(13)$, $^PP_{12}(11)$
$^RR_{12}(15)$, $^PP_{12}(13)$
$^RQ_{11}(13)$, $^PQ_{13}(11)$
$^RQ_{11}(15)$, $^PQ_{13}(13)$
$^RQ_{11}(19)$, $^PQ_{13}(17)$, $^PQ_{33}(3)$ A'7, $^RR(7)$ c11

$^RQ_{11}(17)$, $^PQ_{13}(15)$
$^QQ_{12}(15)$, $^RR(21)$ c12
$^QQ_{12}(21)$, $^RQ_{32}(13)$ A'7
$^QP_{11}(7)$, $^RQ_{12}(29)$ A8
$^OP_{11}(15)$, $^RQ(21)$ c12
$^PP_{12}(17)$, $^RR(23)$ c12

9-0 Band

Ω=1 sub-band

N	$^SR_{31}$	$^RR_{32}$	$^RQ_{31}$	$^QQ_{32}$	$^OP_{31}$	$^PQ_{33}$	$^OP_{33}$
1	8.9		10.5	1.0·	4.0·		
3	11.3·	1.7	16.4·	1.8	10.7	5.4	
5	15.8	2.0·	22.2	2.3	14.2	8.5·	
7	15.8	2.3	24.0·	3.3	19.0	10.0	3.7·
9	15.7	3.0	29.9	4.9	22.5	9.6	5.2·
11	15.5	3.2	26.7	6.2	19.9	7.4	3.7
13	12.5	3.0	21.4	6.5	15.5	5.4	2.0·
15	9.0	2.8·	17.0	6.7	10.2	3.2	
17	5.0·	2.0	12.1	6.4·	6.3	1.9·	
19	3.0	1.4·	8.2	5.4	5.0	1.0·	
21		1.2	5.5	3.0	3.2		
23			3.1	2.1			

$^SR_{31}(3)$, $^PQ_{13}(11)$ A'10
$^SR_{31}(7)$, $^QQ_{22}(19)$ A9
$^SR_{31}(11)$, $^OP_{23}(19)$ A9
$^SR_{31}(17)$, $^QQ_{22}(7)$, $^QQ_{22}(7)$ A8
$^RR_{32}(3)$, $^RQ_{11}(13)$ A'10
$^RR_{32}(5)$, $^QP_{21}(19)$ A9
$^RR_{32}(15)$, $^QQ_{22}(5)$ A8
$^RQ_{11}(15)$, $^QR_{23}(19)$ A8, $^OP_{21}(5)$ A8
$^QQ_{32}(17)$, $^RQ(5)$ c13, $^RR(19)$ c14
$^PQ_{33}(5)$, $^RR_{22}(19)$ A'10, $^PQ(19)$ c15

$^RR_{32}(19)$, $^OP_{12}(11)$ A8
$^RQ_{31}(3)$, $^QQ_{32}(1)$, $^PP(9)$ c14
$^RQ_{31}(7)$, $^PP(19)$ c15
$^QP_{11}(17)$, $^PQ(9)$ c14
$^PQ_{33}(17)$, $^RQ_{21}(13)$
$^PQ_{33}(19)$, $^QP_{12}(27)$ A9
$^PP_{33}(9)$, $^PP_{12}(13)$ A'10
$^OP_{33}(13)$, $^OP_{23}(5)$ A8

Ω=2 sub-band

N	$^SR_{21}$	$^RR_{22}$	$^RQ_{21}$	$^QQ_{22}$	$^OP_{21}$	$^PQ_{23}$	$^PP_{22}$
1	8.0·		9.2	2.0	2.4·		
3	13.7	14.6	13.2	10.7	7.0·		2.1·
5	16.0·	13.9	21.0	15.0	10.0	3.5	4.6
7	19.3	15.5	29.9	19.0·	13.0·	3.2	6.4
9	18.6	13.3	32.3	25.0·	16.5	2.9	6.8
11	20.0·	10.3	32.0	19.1	16.4		5.6·
13	18.0·	6.9	29.1·	14.1	16.2		4.9
15	15.2	4.4	26.6	8.6	15.7		4.0
17	13.0·	3.7	20.0	5.9	12.1		3.2
19	8.9	2.5	16.1	4.5	8.7		1.7
21	6.7	2.1·	9.2·	2.0·	5.7		1.0
23	2.9	1.3	6.9	1.4	3.3		
25			3.1				

$^SR_{21}(1)$, $^QP_{32}(1)$ A8
$^SR_{21}(11)$, $^QR_{12}(9)$ A8
$^SR_{12}(13)$, $^QP_{21}(11)$ A8
$^SR_{21}(17)$, $^PP_{12}(15)$
$^RR_{22}(1)$, $^QQ_{11}(9)$ A8
$^RR_{22}(21)$, $^QQ_{12}(15)$
$^RQ_{11}(21)$, $^PP(1)$ c13
$^RQ_{11}(21)$, $^OP_{11}(15)$
$^SR_{21}(5)$, $^QQ_{22}(1)$ A8, $^SR_{21}(5)$ A8
$^QP_{21}(7)$, $^QR_{23}(7)$ A8, $^QP_{21}(7)$ A8

$^QQ_{22}(9)$, $^PP(17)$ c14
$^QQ_{22}(21)$, $^SR_{31}(9)$ A'8
$^OP_{21}(1)$, $^QQ_{33}(3)$ A8
$^OP_{21}(3)$, $^RQ_{12}(23)$ A8
$^PP_{22}(3)$, $^QR_{12}(23)$ A9
$^PP_{22}(11)$, $^RQ(7)$ c13
$^PP_{22}(15)$, $^PQ(11)$ c13

Ω=3 sub-band

N	$^SR_{11}$	$^RR_{12}$	$^RQ_{11}$	$^QQ_{12}$	$^OP_{11}$	$^PQ_{13}$	$^PP_{12}$
5	1.3·	1.5					
7	2.3·	3.0·	2.7	3.1			
9	2.5·	4.2	3.8	5.4	2.7		
11	2.8	4.0·	4.7·	6.3	2.7	1.8	1.6
13	3.6	3.9	4.9	6.2·	2.5·	2.5	3.2
15	2.9	3.6·	5.1	6.1·	2.2·	2.3	2.2
17	1.6·	3.2	4.6	5.7	1.7	2.1	2.5
19	2.1·	2.3	2.9	4.0	1.2·		1.8·
21	0.8·						

$^SR_{11}(5)$, $^RQ(9)$ c13
$^SR_{11}(9)$, $^QR_{23}(15)$ A8
$^SR_{11}(21)$, $^RR_{32}(13)$ A8
$^RR_{12}(15)$, $^QR_{12}(17)$ A8
$^RR_{12}(11)$, $^QR_{12}(17)$ A8
$^RR_{12}(15)$, $^OP(15)$ c13
$^SR_{11}(17)$, $^QP_{31}(1)$ A'8, $^RR(17)$ c13

$^RQ_{11}(11)$, $^QQ_{11}(17)$ A8
$^QQ_{12}(13)$, $^QR_{12}(19)$ A8
$^QP_{11}(19)$, $^PP(19)$ c13
$^PP_{12}(13)$, $^PQ(23)$ c14
$^PP_{12}(19)$, $^SR_{21}(3)$ A'8

10-0 Band

Ω=1 sub-band

N	$^SR_{31}$	$^RR_{32}$	$^RQ_{31}$	$^QQ_{32}$	$^OP_{31}$	$^PQ_{33}$	$^OP_{33}$
1	7.7		12.2		3.5		
3	13.7	1.3	19.6		7.8	7.1	
5	14.7	2.8	26.4		14.1	8.5	4.3
7	16.3	3.2	31.4	1.9	16.6	9.6·	4.0·
9	15.4·	4.0·	30.7	5.6	17.3	8.5·	4.2
11	15.2	4.3	25.8	6.2	13.4	7.7	3.6·
13	13.5·	4.1	21.8	8.9	10.8	6.2	3.2
15	11.4·	3.8	18.4·	7.0	7.6	3.6	2.5
17	7.5·	2.4	14.0	6.3·	5.5·	2.4	
19	4.3	2.4	7.7	5.0·	4.1		0.5·
21	2.2	1.7	3.7	4.2·	2.6		0.3·
23			1.6	2.5			

$^SR_{31}(9)$, $^PP_{22}(15)$ A'11
$^SR_{31}(13)$, $^QR_{12}(13)$ A9
$^SR_{11}(15)$, $^SR_{21}(7)$
$^RR_{32}(9)$, $^OP_{31}(7)$, $^RR(5)$ c15
$^RQ_{11}(15)$, $^QP_{21}(19)$ A'11
$^QQ_{32}(11)$, $^QQ_{11}(3)$ A9
$^QQ_{32}(17)$, $^PQ_{23}(11)$
$^SR_{31}(17)$, $^QQ_{11}(11)$ A9, $^QP_{32}(11)$ A9
$^PQ_{33}(9)$, $^RR_{12}(13)$ A'11, $^RR(7)$ c15

$^QQ_{32}(19)$, $^PQ(3)$ c14
$^QP_{31}(17)$, $^PR_{21}(15)$ A9
$^PQ_{33}(7)$, $^QP_{11}(11)$ A'11
$^OP_{31}(11)$, $^OP_{23}(19)$, A10
$^OP_{33}(19)$, $^RR_{12}(11)$
$^OP_{33}(21)$, $^PQ(11)$ c14

Ω=2 sub-band

N	$^SR_{21}$	$^RR_{22}$	$^RQ_{21}$	$^QQ_{22}$	$^OP_{21}$	$^PQ_{23}$	$^PP_{22}$
1	8.6·	13.1	7.3		1.5·		
3	15.1	14.7	14.0	11.5·	8.0·		
5	21.0·	16.9	22.0	18.4	13.3	5.8	4.6·
7	24.0	17.0	30.1	19.9	14.1	3.8	6.1
9	24.4·	14.1	39.0	21.0·	17.0·	3.5	7.2
11	23.0	10.2	38.9	15.8	16.0	2.0·	6.6
13	20.8	8.4	35.1	12.5·	14.7	1.5·	5.9
15	18.5	6.5	28.6	11.0	10.5·		3.9
17	12.2·	3.6	18.0·	9.1	11.6		2.9
19	7.7	2.2·	11.0	4.4	9.5·		
21	3.8		8.9	2.0	4.1		
23			5.3		2.9		

$^SR_{21}(1)$, $^QR_{12}(5)$ A9
$^SR_{21}(9)$, $^SR_{21}(21)$ A'11
$^SR_{21}(17)$, $^PP(5)$ c14
$^RQ_{11}(15)$, $^QR_{23}(21)$ c16
$^QQ_{22}(3)$, $^QP_{32}(7)$ A9
$^QQ_{22}(9)$, $^QR_{12}(11)$ A9
$^QQ_{22}(13)$, $^PQ(15)$ c15
$^QP_{21}(1)$, $^RQ_{11}(15)$ A'11
$^RR_{22}(7)$, $^PQ_{13}(15)$ A'11, $^QQ_{33}(9)$ A9
$^RR_{22}(19)$, $^QQ_{33}(5)$ A'9, $^PQ(19)$ c15

$^QP_{21}(3)$, $^QQ_{33}(7)$ A9
$^QP_{21}(9)$, $^QQ_{11}(11)$ A9
$^QP_{21}(11)$, $^QP_{32}(23)$ A10
$^QP_{21}(15)$, $^RQ_{12}(9)$
$^QP_{21}(19)$, $^QR_{12}(11)$
$^PQ_{23}(13)$, $^QQ_{22}(15)$ A9
$^PP_{22}(5)$, $^QP_{12}(7)$ A9
$^PP_{22}(15)$, $^PP(17)$ c15

Ω=3 sub-band

N	$^SR_{11}$	$^RR_{12}$	$^RQ_{11}$	$^QQ_{12}$	$^OP_{11}$	$^PQ_{13}$	$^PP_{12}$
7	2.0·	2.9	1.5·	2.5	1.7		
9	2.5	4.9	5.4	4.4	3.9·		2.4
11	2.9	5.6·	5.2	5.2	3.1·	1.8·	2.0·
13	4.0	5.2	6.0·	5.7	2.5	1.9	
15	3.1	5.4·	6.3	6.0	2.1	2.4·	3.0·
17	2.0	3.8	4.7	5.2	1.4	2.2·	
19		3.6	2.8	4.2	1.4	2.1	1.3

$^SR_{11}(7)$, $^QQ_{33}(15)$ A9
$^RQ_{11}(7)$, $^RQ(1)$ c14
$^RQ_{11}(13)$, $^RR_{32}(3)$ A'9
$^QP_{11}(11)$, $^RR(9)$ c14
$^PQ_{13}(17)$, $^QR_{23}(3)$ A8, $^QP_{21}(3)$ A8

$^PQ_{13}(11)$, $^SR_{31}(3)$ A'9
$^PP_{12}(11)$, $^QP_{12}(17)$ A9
$^PP_{12}(15)$, $^OP_{33}(9)$ A'9

tion of the extra lines is far from negligible for the calculation of the band oscillator strength.

The quality of the present new data is illustrated in Fig. 2 in which integrated cross-section values for the $^QQ_{11}$, $^OP_{32}$, and $^QQ_{22}$ lines in the A–X (5–0) band are presented. The variation of the values with N'' is smooth and regular and provides a

TABLE 1c—*Continued*

11-0 Band

Ω=1 sub-band

N	$^SR_{31}$	$^RR_{32}$	$^RQ_{31}$	$^QQ_{32}$	$^QP_{31}$	$^PQ_{33}$	$^OP_{33}$	$^PP_{32}$
1	7.3		8.8					
3	12.9		13.7			5.9	3.6	
5	13.0		17.5	3.2	7.8	7.2	4.2	
7	15.9		21.6	4.2	10.1	6.3	4.9*	
9	16.2		21.0*	4.3	12.6	5.6	4.6	
11	12.7	4.1	20.3	4.8*	13.0*	4.9	3.2*	6.9*
13	10.0*		18.0*	7.1	7.7	3.5*	2.5	5.1
15	6.4*	1.9	15.3	6.9	5.6			4.8
17			10.0*				2.3	5.0
19			5.8*					

$^SR_{31}(13)$, $^RR_{22}(3)$
$^SR_{31}(15)$, $^QP_{31}(11)$ A10
$^RQ_{31}(17)$, $^QP_{12}(13)$ A10
$^RQ_{31}(19)$, $^RR_{22}(15)$
$^QQ_{32}(7)$, $^QQ_{33}(15)$ A11
$^RQ_{31}(9)$, $^QQ_{11}(1)$ A10, $^QQ_{33}(3)$ A10
$^RQ_{31}(13)$, $^PP(3)$ c16, $^QR_{23}(9)$ A10, $^QP_{21}(9)$ A10
$^QP_{31}(11)$, $^SR_{21}(1)$, $^RQ_{21}(15)$ A'12

$^QQ_{32}(11)$, $^RR_{22}(15)$ A'12
$^PQ_{33}(13)$, $^QP_{12}(11)$ A10
$^OP_{33}(7)$, $^PQ(9)$ c17
$^OP_{33}(11)$, $^QQ_{11}(9)$ A10
$^PP_{32}(11)$, $^PQ(15)$ c18

Ω=2 sub-band

N	$^SR_{21}$	$^RR_{22}$	$^RQ_{21}$	$^QQ_{22}$	$^QP_{21}$	$^PQ_{23}$	$^PP_{22}$
1	8.0*	12.7					
3	14.1	12.0*	14.3	11.1			2.4
5	14.8	13.9	21.1	17.0	7.5	3.5	3.8
7	18.5	13.6*	26.9	17.8	11.5		5.6
9	20.0	11.4	31.3	17.8	13.4	2.7	6.1
11	19.1	9.1	30.1	14.9	13.3	2.0	6.8
13	17.2	7.7	29.2	11.1	14.3		5.1
15	13.7*	5.4*	20.3	7.9	9.0*		3.3*
17	9.3	3.1	17.4	5.7	6.0		
19	6.0		14.4		6.0*		1.8*
21	3.0*		9.7		1.0*	3.4	
23					3.3		

$^SR_{21}(9)$, $^QP_{32}(11)$ A10
$^SR_{21}(15)$, $^QQ_{12}(7)$
$^SR_{21}(21)$, $^SR_{21}(9)$ A'10
$^RR_{22}(7)$, $^QP_{23}(11)$ A11
$^QQ_{22}(21)$, $^PQ13(17)$
$^RQ_{21}(17)$, $^SR_{11}(13)$, $^QP_{23}(17)$ A10
$^QP_{21}(23)$, $^RR(3)$ c14, $^PP(21)$ c16

$^QP_{21}(15)$, $^QR_{23}(17)$ A10
$^QP_{21}(19)$, $^QQ_{12}(15)$
$^PQ_{23}(11)$, $^RQ_{11}(3)$
$^PP_{22}(15)$, $^SR_{11}(9)$ A'10
$^PP_{22}(19)$, $^RQ_{31}(15)$ A'10

Ω=3 sub-band

N	$^SR_{11}$	$^RR_{12}$	$^RQ_{11}$	$^QQ_{12}$	$^QP_{11}$	$^PQ_{13}$	$^PP_{12}$
3			1.0*				
5		1.9	2.1				
7	1.3*	3.0*	4.4	2.0*	3.1		
9	2.2	3.3	3.4	3.1*	3.4		1.7
11	2.5	3.2	4.2	4.9	2.8*		3.1
13	3.0*	3.0*	4.5*	5.2	2.2	2.0	2.0
15	2.5*	2.9	3.4*	4.5*	1.8	2.4*	2.5*
17		2.7*	4.5*	1.0*	1.5*	2.6	

$^SR_{11}(7)$, $^RQ(17)$ c17
$^SR_{11}(15)$, $^QP_{21}(3)$ A9
$^RR_{12}(7)$, $^PP_{22}(19)$ A'12
$^RR_{12}(11)$, $^PP(1)$ c15
$^RQ_{11}(13)$, $^RQ(7)$ c15
$^RQ_{11}(15)$, $^QP_{21}(1)$ A'10
$^RR_{12}(13)$, $^PQ_{33}(9)$ A'10, $^RR(7)$ c15
$^PQ_{13}(15)$, $^RR_{22}(7)$ A'10, $^QQ_{33}(9)$ A9

$^RQ_{11}(17)$, $^RR(19)$ c16
$^QQ_{12}(9)$, $^QQ_{33}(17)$ A10
$^QQ_{12}(17)$, $^OP_{23}(21)$ A10
$^QP_{11}(11)$, $^PQ_{33}(7)$ A'10
$^QP_{11}(17)$, $^SR_{21}(13)$ A9
$^PP_{12}(15)$, $^QP_{32}(9)$ A9

12-0 Band

Ω=1 sub-band

N	$^SR_{31}$	$^RR_{32}$	$^RQ_{31}$	$^QQ_{32}$	$^QP_{31}$	$^PQ_{33}$	$^OP_{33}$
1	6.2		4.7				
3	10.3		8.8		2.1	2.8*	
5	10.0		14.2		7.5	3.5	5.3
7	7.7		17.3*		7.5	3.0	5.2*
9			18.8		6.6	2.0*	2.6
11					5.1		

$^RQ_{31}(7)$, $^SQ_{31}(5)$ A11
$^QP_{31}(5)$, $^RQ(5)$ c19
$^QP_{31}(7)$, $^QR_{23}(3)$ A11, $^QP_{21}(3)$ A11
$^PQ_{33}(9)$, $^QR_{23}(7)$ A11, $^QP_{21}(7)$ A11

$^PQ_{33}(3)$, $^PP(3)$ c19
$^OP_{33}(7)$, $^PQ(7)$ c19

Ω=2 sub-band

N	$^SR_{21}$	$^RR_{22}$	$^RQ_{21}$	$^QQ_{22}$	$^QP_{21}$	$^PQ_{23}$	$^PP_{22}$
1	7.0		5.2				
3	10.9	10.7	10.2				
5	11.0	15.6	17.8	17.0	7.3		
7	12.5	11.3	18.8	14.3	7.9	3.3	
9	15.3	8.8	18.0*	12.0	8.3	2.5*	2.2*
11	11.7	7.8	17.5	10.2	9.8		4.5*
13	9.3	5.5*	15.0*	6.8	8.0*		3.8
15	8.5	4.5*	12.0*	2.8	6.0		
17				2.6	4.7		
19							1.7*

$^RR_{22}(13)$, $^QR_{12}(15)$ A11
$^RR_{22}(15)$, $^QQ_{32}(11)$ A'11
$^QP_{21}(13)$, $^QQ_{22}(1)$ A10
$^SR_{21}(5)$, $^QR_{23}(9)$ A11, $^QP_{21}(9)$
$^RQ_{21}(9)$, $^RQ(3)$ c17, $^QP_{23}(11)$ A11
$^RQ_{21}(13)$, $^SQ_{31}(3)$ A10, $^QQ_{11}(15)$ A11
$^RQ_{21}(15)$, $^QP_{31}(11)$ A'11, $^SR_{21}(1)$ A'11

$^QP_{21}(15)$, $^OP_{12}(7)$ A10
$^PQ_{23}(9)$, $^QQ_{33}(13)$ A11
$^PP_{22}(9)$, $^QP_{32}(13)$ A11
$^PP_{22}(11)$, $^OP_{12}(13)$ A11
$^PP_{22}(19)$, $^RR_{12}(7)$ A'11

Ω=3 sub-band

N	$^SR_{11}$	$^RR_{12}$	$^RQ_{11}$	$^QQ_{12}$	$^QP_{11}$	$^PQ_{13}$	$^PP_{12}$
5		3.0					
7	1.3	3.1	1.9				
9		3.3	2.8*	3.7*	1.4		
11	2.8	2.1	2.7	3.8*	2.0		
13	2.3	2.5	2.5*	3.8*	2.6*		
15	2.8	2.0*	3.8				
17		1.7	1.5	2.3	0.8		

$^RR_{12}(15)$, $^QR_{12}(13)$ A10
$^RQ_{11}(9)$, $^QR_{12}(15)$ A11
$^RQ_{11}(13)$, $^OP_{23}(9)$ A10
$^QQ_{12}(11)$, $^PP(1)$ c16, $^RQ(17)$ c18, $^PP(15)$ c18
$^QP_{11}(13)$, $^QR_{23}(11)$ A10, $^QP_{21}(11)$ A10

$^RQ_{11}(15)$, $^QQ_{11}(13)$ A10
$^QQ_{12}(13)$, $^QR_{12}(11)$ A10

---

good data set for the calculation of the band oscillator strengths. For comparison, the values of Yoshino *et al.* (*10*) are also indicated.

II. Band Oscillator Strengths

In absorption at ambient temperature (293 K), bands are only observed with $v'' = 0$ for the Herzberg transitions. The relative population N_0 of this level is assumed to be 1.00. Therefore the band oscillator strength $f_{v,0}$ for the (*v*–0) bands is calculated using the formula

$$f_{v,0} = \frac{mc^2}{\pi e^2 N_0} \int_{band} \sigma(\nu)d\nu = 1.130 \times 10^{12} \int_{band} \sigma(\nu)d\nu,$$

[1]

where the integral is equal to the sum of the integrated cross sections of all the lines in the band. The other parameters have their usual meanings (*m* and *e*: electronic mass and charge; *c*: velocity of light).

A–X transition. Table 2a gives the integrated cross sections and the band oscillator strengths for the A–X bands. As mentioned above, some lines in the bands with $v' = 8$–10 are saturated. For these lines, integrated cross sections were calculated by fitting the lines of the band to the model of Bellary and Balasubramanian (*27*) (see next section). For the perturbed (11–0) band, the intensities of extra lines were taken into account. The accuracy as defined previously for the integrated line cross section (in percent) is given for each band. Table 2a also gives the values of Hasson *et al.* (*14*), the recommended values of Huestis *et al.* (*7*), and the values of Yoshino *et al.* (*10*). Our values are in good agreement with those of Hasson *et al.* (*14*) and Yoshino *et al.* (*10*), except for the (11–0) band which, in this work, includes extra lines not observed (or unassigned) by the latter authors. Our values are slightly lower than most of the recommended values of Huestis *et al.* (*7*) and for the bands with $v' = 0$, 1, and 11, they are clearly lower. The values recommended by Huestis *et al.* (*7*) were obtained by referring to the values of Hasson *et al.* (*14*) for the (7–0) band and by accepting that the Frank–Condon factors represent the relative transition strengths. The value thus obtained for the
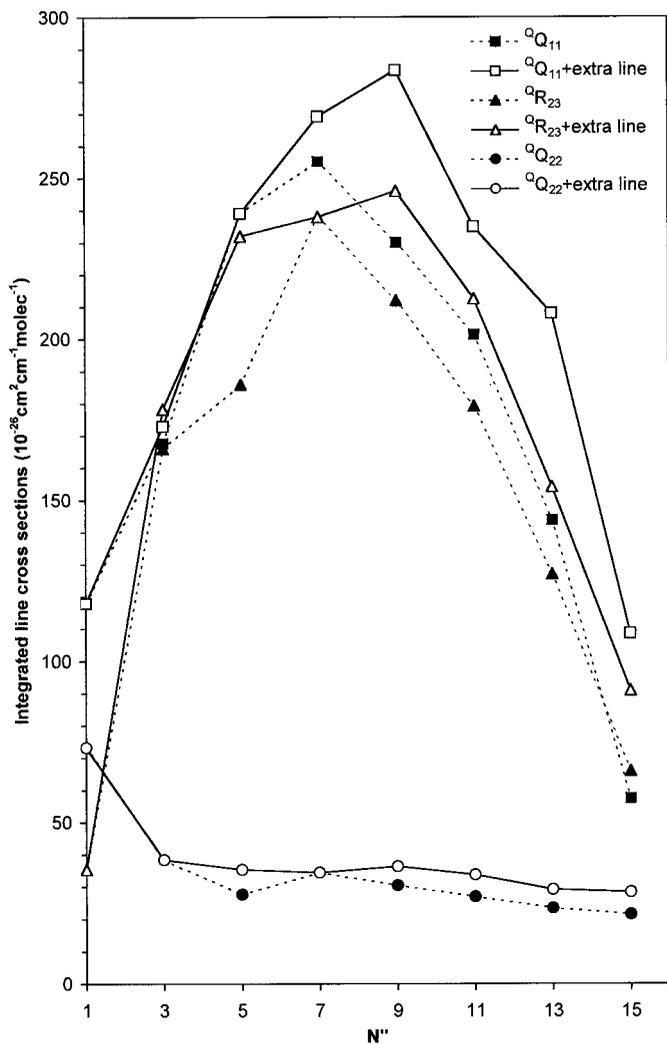
FIG. 1. Integrated line cross sections in the perturbed $A–X$ (11–0) band, with and without the extra lines arising from the interaction of the $A^3\Sigma_u^+$, $v =$ 11 with a $^3\Pi_u$ state (see text and Ref. (*13*)).

(7–0) band is about 2% larger than ours and than that of Yoshino *et al.* (*10*); the differences for the other bands are therefore limited to this discrepancy, as was already pointed out by Yoshino *et al.* (*10*). For the (0–0) and (1–0) bands, the differences probably result from the fact that these bands are weak in our spectra and, thus, that a limited number of lines are observed. Finally, it can be noted that the values of Bao *et al.* (*19*), obtained by laser absorption measurements in the (8–0) and (9–0) bands, show large discrepancies with all other results.

c–X transition. The values for the integrated cross sections and band oscillator strengths of the *c–X* transition are given in Table 2b. Comparisons are made with the recommended values of Huestis *et al.* (*7*) and with the more recent values of Yoshino *et al.* (*21*). The values derived from Bates (*18*) (not included in Table 2b) are three to four times larger. The values of Huestis

et al. (*7*) were normalized to the recommended values of the $A–X$ transition and are in agreement with our values for the (13–0) and (14–0) bands. For the other bands, although the number of observed lines is roughly the same as in our spectra, significant discrepancies are observed.

Figure 3 shows the variation of the band oscillator strengths of the *c–X* system as a function of v', compared to the recommended values of Huestis *et al.* (*7*) and to the experimental values of Yoshino *et al.* (*21*). A maximum corresponding to $v' = 12$ is found as well for our set as for that of Yoshino *et al.* (*21*), while the recommended values of Huestis *et al.* (*7*) do not show this maximum. Our values are also larger than the experimental values of Yoshino *et al.* (*21*). Due to a smaller path length (122.5 m), the latter authors observed a smaller number of bands ($v' = 7$–16) having a smaller number of lines ($N'' \leq 19$) compared to the present data. Yoshino *et al.* (*21*) corrected their values in order to take into account lines up to
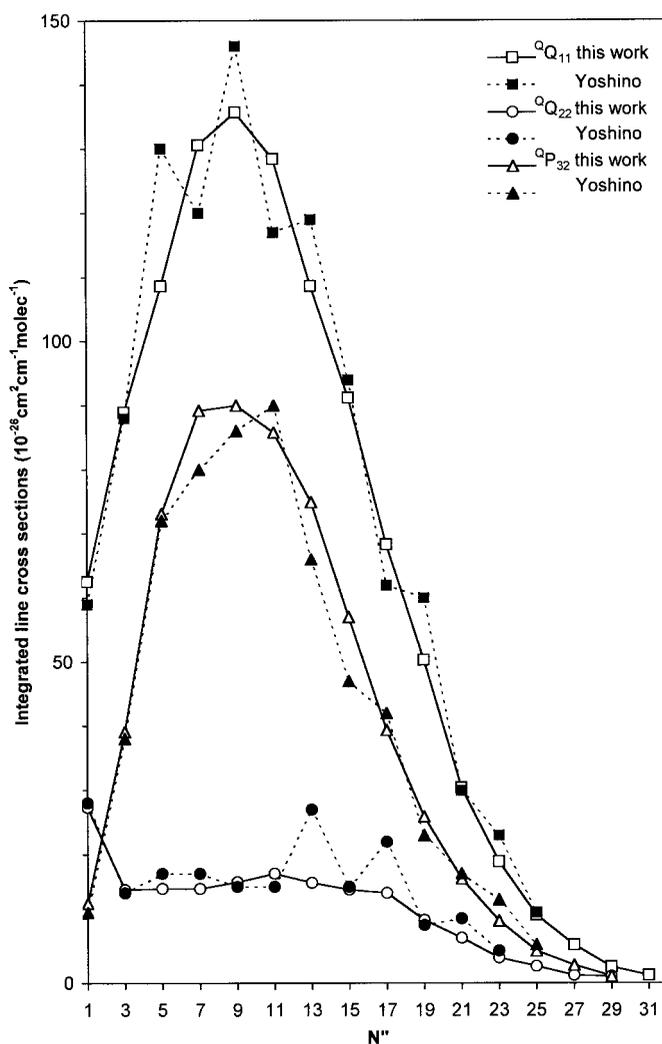
FIG. 2. Integrated cross sections for the $^{Q}Q_{11}$, $^{Q}Q_{22}$, and $^{Q}P_{32}$ lines of the $A–X$ (5–0) band: comparison with the previous values of Yoshino *et al.* (*10*).

TABLE 2a

Integrated Cross Sections and Band Oscillator Strengths
for the A–X (v'–0) Bands of O_2

Band	Integrated cross sections (cm²cm⁻¹molec⁻¹) This work[a]	Band oscillator strengths			
		This work	Hasson[d] (1970)	Huestis[e] (1994)	Yoshino[f] (1995)
0-0	74E-27(12)	8.36E-14	8.53E-14	1.06E-13	
1-0	71E-26(6)	8.02E-13	7.45E-13	8.91E-13	
2-0	33E-25(4)	3.73E-12	3.33E-12	3.85E-12	
3-0	98E-25(3)	1.11E-11	1.03E-11	1.14E-11	
4-0	222E-25(3)	2.51E-11	2.46E-11	2.66E-11	2.43E-11
5-0	45E-24(3)	5.09E-11	4.87E-11	5.14E-11	4.98E-11
6-0	74E-24(3)	8.36E-11	8.34E-11	8.58E-11	8.28E-11
7-0	108E-24(3)	1.22E-10	1.24E-10	1.24E-10	1.22E-10
8-0	139E-24(3)[b]	1.57E-10	1.63E-10	1.60E-10	1.55E-10
9-0	158E-24(3)[b]	1.79E-10	1.85E-10	1.78E-10	1.71E-10
10-0	145E-24(3)[b]	1.64E-10	1.77E-10	1.68E-10	1.65E-10
11-0	81E-24(4)[c]	9.15E-11	1.25E-10	9.93E-11	7.98E-11

[a] The value in parentheses is the estimated percentage accuracy.

[b] Calculated values were taken for the saturated lines (see the text).

[c] Values obtained by the summation of the integrated cross sections of normal and extra lines arising from the interaction with a $^3\Pi_u$ state (see text and Ref. (13)).

[d] Ref. (14).

[e] Recommended values of Ref. (7).

[f] Ref. (10).

TABLE 2b

Integrated Cross Sections and Band Oscillator Strengths
for the c–X (v'–0) Bands of O_2

Band	Integrated cross sections (cm²cm⁻¹molec⁻¹) This work[a]	Band oscillator strengths		
		This work	Huestis[b] (1994)	Yoshino[c] (1999)
2-0	6E-26(25)	6.78E-14		
3-0	20E-26(8)	2.26E-13		
4-0	47E-26(6)	5.31E-13		
5-0	88E-26(5)	9.94E-13		
6-0	148E-26(4)	1.67E-12		
7-0	223E-26(4)	2.52E-12		2.43E-12
8-0	31E-25(4)	3.50E-12		3.18E-12
9-0	40E-25(4)	4.52E-12		3.55E-12
10-0	47E-25(4)	5.31E-12	3.94E-12	4.28E-12
11-0	56E-25(4)	6.33E-12	4.82E-12	4.80E-12
12-0	65E-25(4)	7.35E-12	5.68E-12	5.90E-12
13-0	57E-25(4)	6.44E-12	6.43E-12	5.36E-12
14-0	60E-25(4)	6.78E-12	7.09E-12	5.19E-12
15-0	59E-25(4)	6.67E-12	7.56E-12	4.81E-12
16-0	45E-25(4)	5.09E-12	7.85E-12	4.28E-12
17-0	36E-25(5)	4.07E-12		
18-0	20E-25(6)	2.26E-12		
19-0	84E-26(8)	9.49E-13		

[a] The value in parentheses is the estimated percentage accuracy.

[b] Recommended values of Ref. (7).

[c] Ref. (21).
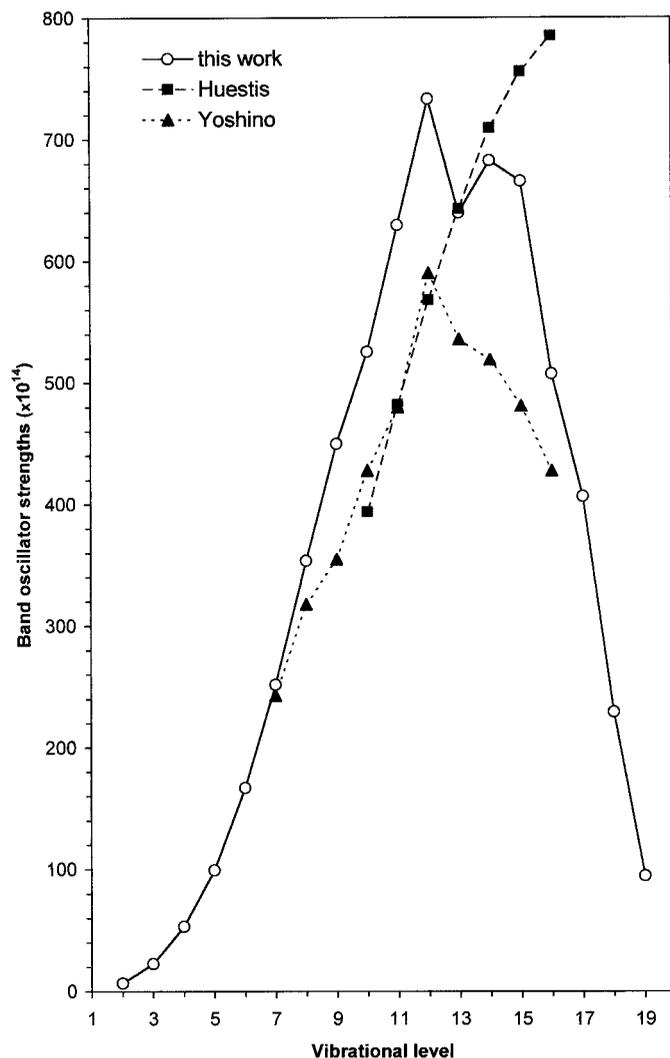
FIG. 3. Band oscillator strengths for the *c–X* transition: comparison with the recommended values of Huestis *et al.* (*7*) and with the recent values of Yoshino *et al.* (*21*).

$N'' = 29$. However, their calculated values of the band oscillator strengths are still lower than ours (Table 2b).

A'–X transition. Table 2c presents the integrated cross sections of the *A'–X* subbands. The calculated band oscillator strengths are compared to the recommended values of Huestis *et al.* (*7*) which, as in the case of the *c–X* transition, were normalized to those of the *A–X* system. The agreement between both sets is within the limit of the estimated error for the (6–0) to (8–0) bands but not for the other bands. Previous values calculated from Bates's data (*18*) are three to four times larger (*7*); those obtained by Kerr and Watson (*23*) from densitometric measurements of photographic plates for the (4–0), (7–0), and (9–0) bands are much smaller (about five times smaller for the (7–0) band).

Figure 4 shows the variation of the integrated cross section with v'. The main contribution to a given band is due to the Ω'

= 2 subbands as proved by the intensity ratios of the different subbands to the total band $I_{\Omega'}/I_{\text{band}}$:

$$I_{\Omega'=1}/I_{\text{band}} \approx 40\%, \quad I_{\Omega'=2}/I_{\text{band}} \approx 50\%, \quad I_{\Omega'=3}/I_{\text{band}} \approx 10\%.$$

III. Transition Moments

A–X transition. Formulas on the line intensities of $^3\Sigma_u^+ - {}^3\Sigma_g^-$ transitions were obtained previously (*7, 28, 29*) and particular attention was devoted to the *A–X* transition of oxygen (*7, 16, 29, 30*). More recently, Bellary and Balasubramanian (*27*) defined 13 parameters for the transition moment of a $^3\Sigma^\pm - {}^3\Sigma^\mp$ transition: three vibronic parallel (*Z*) and perpendicular (*X, Y*) parameters due to spin–orbit interaction, six rovibronic parameters (M_{ef}, M_{fe}, M_1, M_2, N_e, N_f) due to rotation–orbit effects, and four second-order parameters which arise from cross terms involving the preceding interactions. They
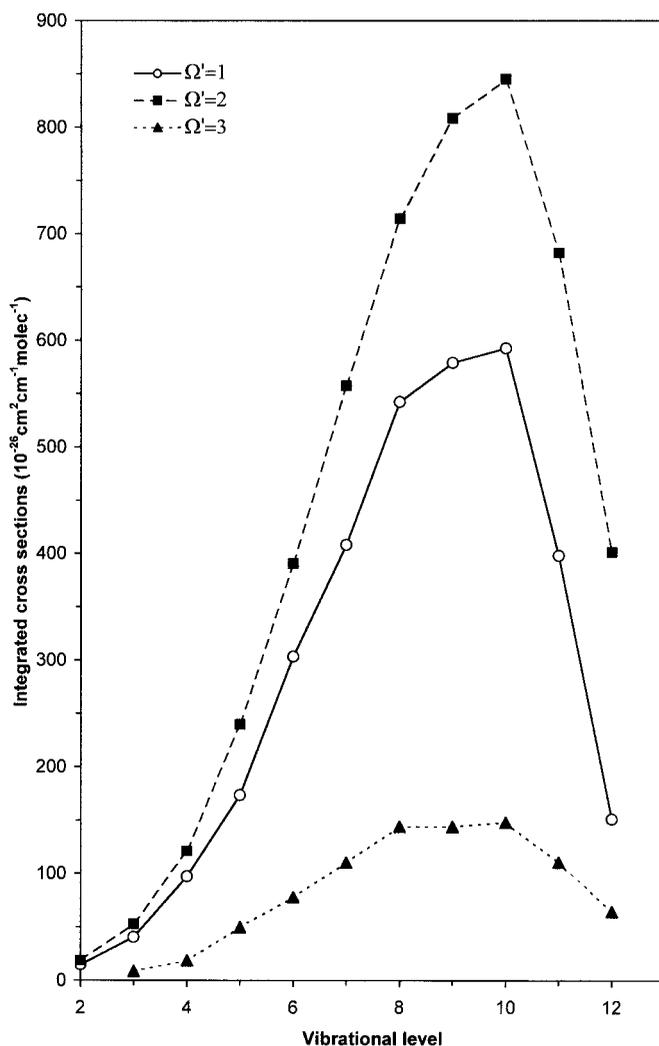
FIG. 4. Integrated cross sections for the *A'–X* (v'–0) subbands with Ω' = 1, 2, and 3.

TABLE 2c
Integrated Cross Sections and Band Oscillator Strengths
for the A'–X (v'–0) Bands of O_2

Band	Integrated cross sections $(cm^2 cm^{-1} molec^{-1})$				Band oscillator strengths	
	This work[a]				This work	Huestis[b] (1994)
	$\Omega=1$	$\Omega=2$	$\Omega=3$	total		
2–0	15E-26	19E-26		34E-26(12)	3.84E-13	
3–0	40E-26	53E-26	9E-26	102E-26(8)	1.15E-12	
4–0	97E-26	121E-26	19E-26	24E-25(6)	2.68E-12	
5–0	174E-26	240E-26	50E-26	46E-25(5)	5.24E-12	
6–0	304E-26	390E-26	78E-26	77E-25(4)	8.72E-12	8.40E-12
7–0	409E-26	558E-26	111E-26	108E-25(4)	1.22E-11	1.25E-11
8–0	542E-26	714E-26	144E-26	140E-25(4)	1.58E-11	1.64E-11
9–0	579E-26	808E-26	144E-26	153E-25(5)	1.73E-11	1.92E-11
10–0	593E-26	845E-26	148E-26	159E-25(6)	1.79E-11	2.02E-11
11–0	398E-26	682E-26	111E-26	119E-25(8)	1.35E-11	1.67E-11
12–0	151E-26	401E-26	65E-26	62E-25(10)	6.97E-12	

[a] The value in parentheses is the estimated percentage accuracy.
[b] Recommended values of Ref. (*7*).

noted that some of the parameters are either equal or negligible depending on the transition studied. England *et al.* (*20*) have used these parameters to fit the intensities measured by Yoshino *et al.* (*10*). They found that only three parameters (Z, X, M) were required, with $X = Y$, and $M = M_1 = M_2 = M_{ef} = M_{fe}$; the other parameters were put to zero without any loss of precision.

Applying the formulas of Bellary and Balasubramanian (*27*) to our data as in the procedure of England *et al.* (*20*), we have determined new values for the transition moment parameters in the following way.

The linestrengths $S_{J'J''}$ were calculated from the integrated line cross sections using the relation

$$f_{v'v'J'J''} = \frac{mc^2}{\pi e^2 N_{J''}} \int_{line} \sigma(\nu)d\nu = \frac{8\pi^2 mc}{3he^2g''} \frac{\nu_{v'v'J'J''} q_{v'v'J'J''}}{2J''+1} S_{J'J''},$$

[2]

where $N_{J''}$ is the relative population of the level ($v'' = 0$, J'') and g'' is the statistical weight of the lower state ($g'' = 3$ for the $X^3\Sigma_g^-$ state). The wavenumbers used in the calculation are

TABLE 3a
Transition Moment Parameters, *r*-Centroid, and Effective Transition Moment (Calculated for $J' = 9$, See Text) for the A–X (v'–0) Bands of O_2

Band	Z $(10^{-4}$ a.u.)	X $(10^{-4}$ a.u.)	M $(10^{-6}$ a.u.)	r-centr. (Å)	M eff. $(10^{-4}$ a.u.)
0–0	7.53(1.00)	4.86(0.45)		1.3490	7.10
1–0	9.06(0.20)	3.63(0.11)	8.8(0.7)	1.3403	6.80
2–0	9.42(0.19)	3.75(0.11)	9.2(0.7)	1.3323	7.06
3–0	9.26(0.15)	3.81(0.08)	9.0(0.5)	1.3251	7.03
4–0	9.26(0.13)	3.74(0.07)	9.1(0.5)	1.3184	6.98
5–0	9.61(0.07)	3.85(0.04)	9.4(0.3)	1.3123	7.21
6–0	9.47(0.12)	3.89(0.06)	9.3(0.4)	1.3068	7.19
7–0	9.62(0.08)	3.84(0.05)	9.8(0.3)	1.3019	7.23
8–0	9.67(0.09)	3.94(0.05)	9.7(0.3)	1.2976	7.32
9–0	9.86(0.08)	3.94(0.04)	9.8(0.3)	1.2939	7.40
10–0	9.84(0.11)	3.92(0.06)	10.0(0.4)	1.2910	7.38
11–0	9.77(0.20)	4.02(0.12)	9.0(1.0)	1.2889	7.40

TABLE 3b
Transition Moment Parameters, *r*-Centroid for the c–X (v'–0) Bands of O_2

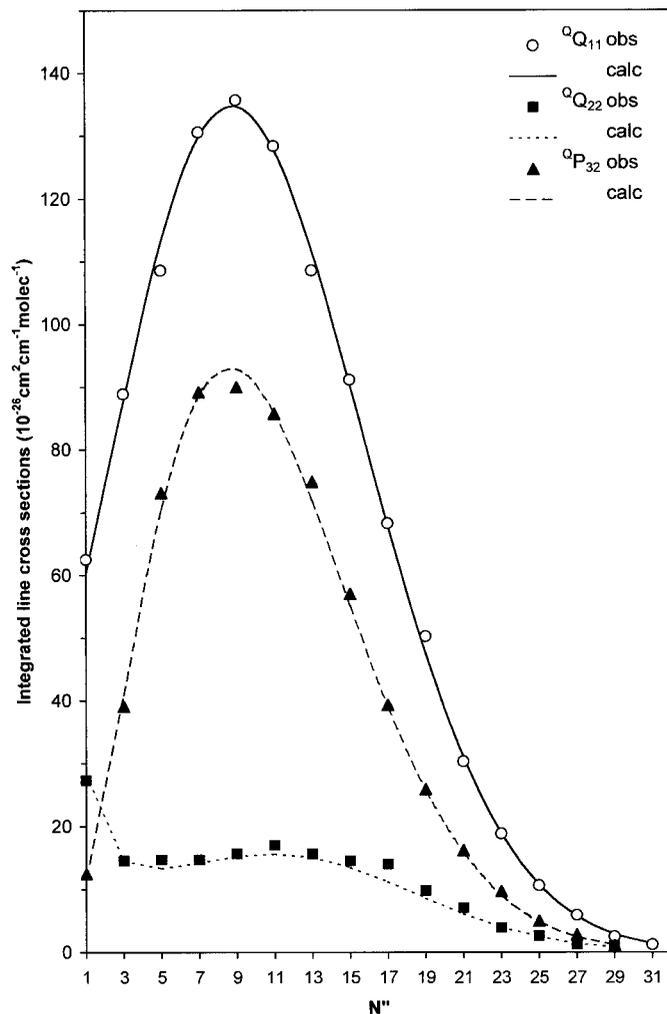| Band	μ $(10^{-4}$ a.u.)	a (10^{-3})	b (10^{-3})	r-centr. (Å)
2–0	1.107(0.034)	5.3(4.6)	8.7(4.4)	1.3298
3–0	1.104(0.015)	4.6(2.0)	8.4(2.0)	1.3224
4–0	1.118(0.011)	3.2(1.4)	7.9(1.3)	1.3155
5–0	1.093(0.010)	3.0(1.3)	7.9(1.3)	1.3092
6–0	1.087(0.005)	2.9(0.6)	8.9(0.6)	1.3034
7–0	1.081(0.006)	2.0(0.8)	9.7(0.8)	1.2981
8–0	1.080(0.010)	1.2(1.4)	9.0(1.3)	1.2932
9–0	1.084(0.009)	2.5(1.2)	9.9(1.2)	1.2888
10–0	1.060(0.008)	2.1(1.0)	10.9(1.0)	1.2849
11–0	1.093(0.008)	2.6(1.1)	9.4(1.1)	1.2813
12–0	1.120(0.038)	7.0(4.8)	7.8(4.7)	1.2781
13–0	1.067(0.009)	4.8(1.2)	8.1(1.2)	1.2754
14–0	1.113(0.015)		9.3(1.9)	1.2730
15–0	1.165(0.016)	3.2(1.9)	11.6(1.9)	1.2710
16–0	1.115(0.014)	3.6(1.8)	8.8(1.7)	1.2694
17–0	1.159(0.017)	2.5(2.2)	11.2(2.2)	1.2681
18–0	1.158(0.025)		9.7(3.5)	1.2673
19–0	1.142(0.090)			1.2667

FIG. 5. Integrated cross sections for the $^QQ_{11}$, $^QQ_{22}$, and $^QP_{32}$ lines of the A–X (5–0) band: experimental values and fitted curves according to the model of Bellary and Balasubramanian (27).

those of Paper I. The Frank–Condon factors $q_{v'v''J'J''}$ were obtained from RKR curves calculated with the molecular constants of Amiot and Vergès (31) for the $X^3\Sigma_g^-$ state and those of Jenouvier et al. (13) for the $A^3\Sigma^+$ state. According to England et al. (20), the variation of $q_{v'v''J'J''}$ with J'' can be represented by a linear function of $J''(J'' + 1)$: $q_{v'v''J'J''} = q_{v'v''}[1 + \beta_{v'v''}J''(J'' + 1)]$. The parameters $q_{v'v''}$ and $\beta_{v'v''}$ obtained by fitting our values to this function are in very good agreement with those of England et al. (20). Using the formulas of Bellary and Balasubramanian (27) for the line strengths $S_{J'J''}$, the best fit of the integrated line cross sections to Eq. [2] is obtained with three parameters (Z, X, M), confirming the results of England et al. (20). The values (in a.u.) of these parameters and the r-centroid values determined from the RKR curves defined above are given in Table 3a. The uncertainty (2σ) in the Z, X, and M parameters is better than that found by England et al. (20), showing the good quality of the line intensity values determined in the present work.

Figure 5 presents, as an example, the fitted curves and the experimental values of the integrated line cross sections for the $^QQ_{11}$, $^QP_{32}$, and $^QQ_{22}$ lines of the (5–0) band.

Figure 6 shows the variation of the Z parameter with the r-centroid value, compared to the values of England et al. (20) and to the values obtained from the U9 parameter defined by Klotz and Peyerimhoff (30) with $Z = \sqrt{2}$ U9 (see footnote 8 of (20)). For comparison the error bars corresponding to the uncertainty (3σ) given by England et al. (20) have been readjusted to the uncertainty values (2σ) given in our work.

Table 3a also gives the values obtained for the effective transition moment defined according to Buijsse et al. (32):

$$M_{\text{eff}}^2 = [Z^2 + 4Y^2 - 4M + 6M^2J''(J'' + 1)]/g''. \quad [3]$$

TABLE 3c
Transition Moment Parameters, r-Centroid, and Effective Transition Moment
(Calculated for $J' = 9$, See Text) for the A'–X (v'–0) Bands of O_2

Band	Z_1 (10^{-5} a.u.)	X_1 (10^{-6} a.u.)	Y_1 (10^{-4} a.u.)	X_2 (10^{-6} a.u.)	Y_2 (10^{-4} a.u.)	X_3 (10^{-6} a.u.)	r-centr. (Å)	M eff. (10^{-4} a.u.)
2–0	−2.0 (1.1)	4.0 (0.8)	1.24 (0.09)	4.6 (0.5)	1.47 (0.08)		1.3294	2.10
3–0	−2.9 (0.6)	3.4 (0.5)	1.27 (0.05)	4.9 (0.3)	1.39 (0.05)	5.2 (0.5)	1.3221	2.18
4–0	−2.4 (0.5)	3.3 (0.4)	1.34 (0.04)	4.8 (0.2)	1.42 (0.04)	5.0 (0.4)	1.3154	2.22
5–0	−2.3 (0.5)	3.1 (0.3)	1.32 (0.04)	4.9 (0.2)	1.42 (0.04)	5.3 (0.3)	1.3092	2.22
6–0	−1.9 (0.5)	3.3 (0.3)	1.34 (0.04)	5.0 (0.2)	1.44 (0.04)	5.3 (0.3)	1.3037	2.25
7–0	−1.8 (0.4)	3.4 (0.3)	1.31 (0.03)	4.9 (0.2)	1.45 (0.03)	5.3 (0.3)	1.2987	2.24
8–0	−1.6 (0.5)	3.3 (0.3)	1.32 (0.04)	4.9 (0.2)	1.47 (0.03)	5.2 (0.3)	1.2943	2.25
9–0	−1.8 (0.6)	3.4 (0.4)	1.29 (0.05)	5.0 (0.3)	1.45 (0.05)	5.3 (0.5)	1.2904	2.23
10–0	−0.9 (0.6)	3.5 (0.4)	1.31 (0.05)	5.3 (0.3)	1.49 (0.04)	5.4 (0.4)	1.2872	2.28
11–0	1.1 (0.7)	3.9 (0.5)	1.15 (0.05)	5.1 (0.3)	1.47 (0.04)	5.2 (0.5)	1.2847	2.17
12–0	0.9 (1.3)	3.7 (1.4)	1.04 (0.10)	3.6 (0.4)	1.36 (0.06)	4.6 (0.7)	1.2828	1.95
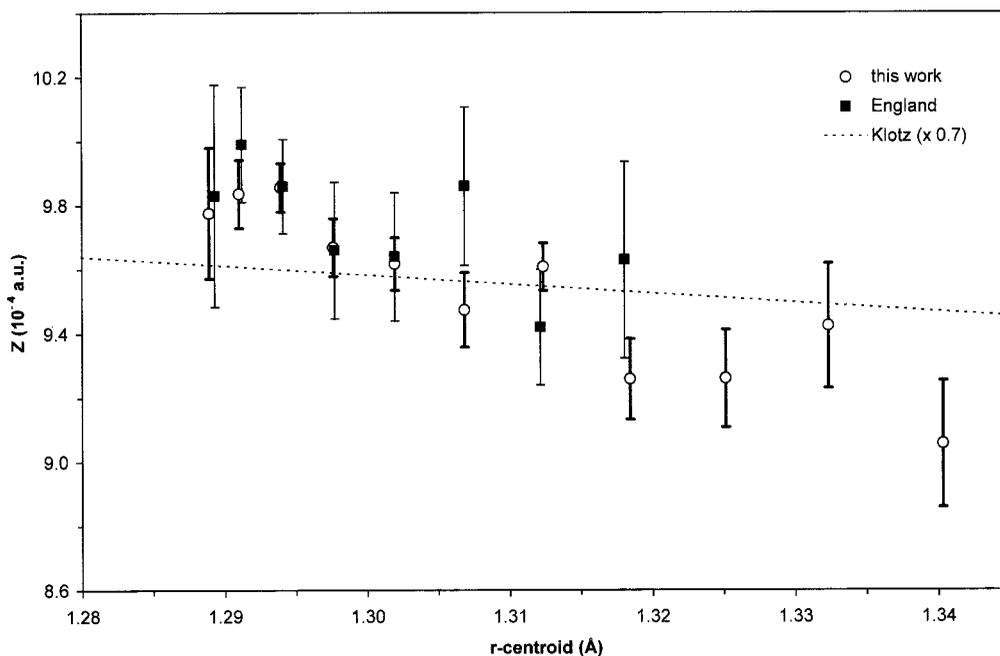
FIG. 6. Electronic transition moment for the A–X (v'–0) bands ($v' = 0$–11): this work; the values of England *et al.* (*20*) derived from the experimental data of Yoshino *et al.* (*10*); the curve derived from the ab initio calculations of Klotz and Peyerimhoff (*30*) after normalization and adjustment for comparison (see text).

These values were calculated for $J'' = 9$, corresponding to the strongest lines at the temperature (293 K) of our experiments, and can be fitted to an r-centroid linearly dependent relation (*32*) valid in the region 1.28 Å $< r <$ 1.34 Å:

$$M_{\mathrm{eff}} = (21.24\text{–}10.73r)10^{-4} \text{ a.u.} \qquad [4]$$

The coefficients of this relation are close to those determined by Buijsse *et al.* (*32*): $M_{\mathrm{eff}} = (21.54\text{–}11.12r)10^{-4}$ a.u. at 300 K.

c–X transition. The relations giving the line intensities in a $^1\Sigma$–$^3\Sigma^-$ transition were first derived by Watson (*33*). In this model, the linestrengths are dependent on a single transition moment μ. First-order spin–orbit interactions between the $c\,^1\Sigma_u^-$ state and a $^3\Pi_u$ state and between the $X\,^3\Sigma_g^-$ state and a $^1\Pi_g$ state were shown (*30*) to allow this otherwise forbidden transition to occur.

Using the rotational linestrengths of Watson (*33*), we tried to derive the transition moment μ for each band: the standard deviation obtained was quite satisfactory but the calculated intensities for the lines in the branches showed increasing discrepancies with the observed ones as N'' increases, especially for the ^RQ and ^PQ branches, which showed discrepancies of opposite signs. To eliminate these deviations, factors $(1 \pm aJ'')$ for the ^PP and ^RR lines and $(1 \pm bJ'')$ for the ^RQ and ^PQ lines were introduced into the original linestrength formulas of Watson (*33*). A similar approach was adopted by Bellary and Balasubramanian (*34*) to fit the intensities in the branches of

the $a\,^1\Delta_g$–$X\,^3\Sigma_g^-$ transition of oxygen. Table 3b gives the values for the a, b, and μ parameters and their uncertainty (2σ). The μ values are only slightly different from those obtained in our first calculations fitting the intensities to Watson's model (*33*), but the standard deviation is improved. The r-centroids are determined from the potential curves calculated with the molecular parameters of Paper I for the c state and of Amiot and Vergès (*31*) for the X state. In Figs. 7a (for the ^RR and ^PP branches) and 7b (for the ^RQ and ^PQ branches), the observed integrated line cross sections of the c–X (11–0) band are compared to the calculated values obtained with the model of Watson (*33*) and with the modified formulas. Figure 8 shows the variation of the μ parameter with r, compared to the values of Klotz and Peyerimhoff (*30*) and of Buijsse *et al.* (*32*). The values of Klotz and Peyerimhoff are greater by about a factor of 2. To present all three sets of values on the same graph, the values of Klotz and Peyerimhoff (*30*) presented in Fig. 8 have been multiplied by 0.6.

A′–X transition. To account for the intensities in the A'–X transition, Kerr and Watson (*23*) worked out a model with six transition moment parameters; three of them (Z_1, Y_1, and Y_2) arise from first-order spin–orbit interactions, and the three others (X_1, X_2, X_3) from low-order orbit–rotation couplings. From densitometric measurements of the intensities of the (4–0), (7–0), and (9–0) bands, these authors estimated the values of these parameters. For X_3, they gave only the value for the (7–0) band. Huestis *et al.* (*7*) defined a single set of six relative parameters for all v' values of the A'–X (v'–0) bands.
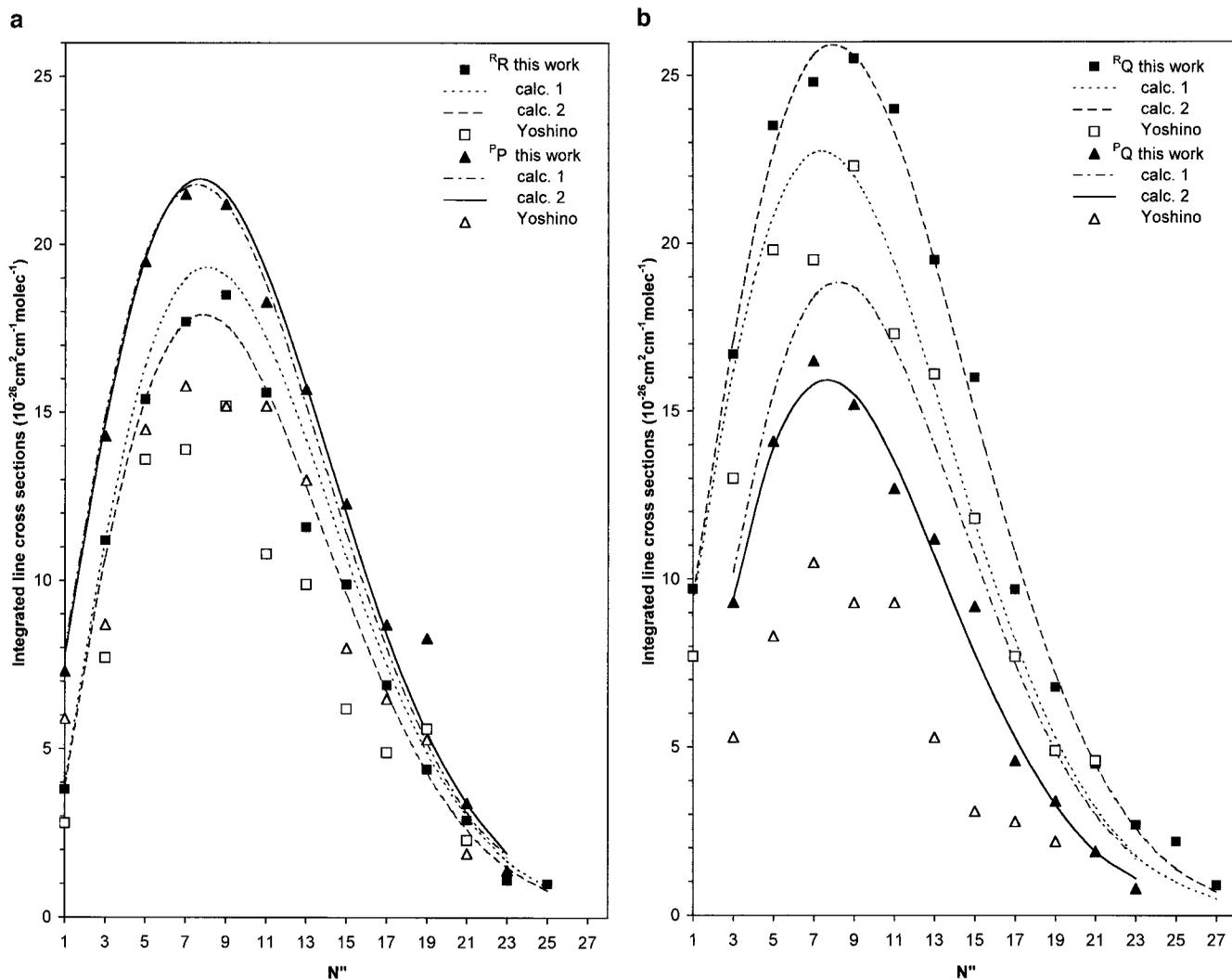
FIG. 7. (a) Integrated line cross sections in the ^RR and ^PP branches of the c–X (11–0) band: this work; fitted curve according to the model of Watson (*33*); fitted curve derived from a modified model (see text); experimental data of Yoshino *et al.* (*21*). (b) Integrated line cross sections in the ^RQ and ^PQ branches of the c–X (11–0) band: this work; fitted curve according to the model of Watson (*33*); fitted curve derived from a modified model (see text); experimental data of Yoshino *et al.* (*21*).

The ratios of these parameters are in agreement with those obtained from the values of Kerr and Watson (*23*).

Using the results of the ab initio calculations of Klotz and Peyerimhoff (*30*) and the values of the CRDS oscillator strengths of Huestis *et al.* (*7*) for the (9–0) and (11–0) bands, Buijsse *et al.* (*32*) deduced a linear *r*-centroid dependence of the effective electronic transition moment, valid for room-temperature conditions. They also derived a formula for a temperature of 5–10 K, corresponding to a total population in the $J'' = 0$ level.

In the present work, we used the model of Kerr and Watson (*23*) to fit the intensities of the lines in the A'–X bands. Figures 9a, 9b, and 9c present the averaged differences (in percent) between the observed and calculated integrated cross sections for the branches of each observed (v'–0) subband. The inten-

sities are fairly well represented by this model for most of the branches, but, as already shown by Kerr and Watson (*23*), large discrepancies are observed for some of them: $^OP_{33}$, $^RR_{32}$, and $^QQ_{32}$ branches in Fig. 9a; $^PQ_{23}$ and $^QP_{21}$ branches in Fig. 9b; $^QP_{11}$ branches in Fig. 9c. To improve the fits, additional higher order terms were introduced according to Bellary and Balasubramanian (*35*), but the results were only slightly affected by these additions. It is evident that the formulas proposed for some of the branches are still inappropriate. Nevertheless, the parameters defined by Kerr and Watson (*23*) and calculated from the present data are given in Table 3c, together with their uncertainty (2σ). As expected, their ratios are in agreement with those derived from Kerr and Watson (*23*) for the (4–0), (7–0), and (9–0) bands. The two larger parameters Y_1 and Y_2 are represented in Fig. 10, where they are compared to the
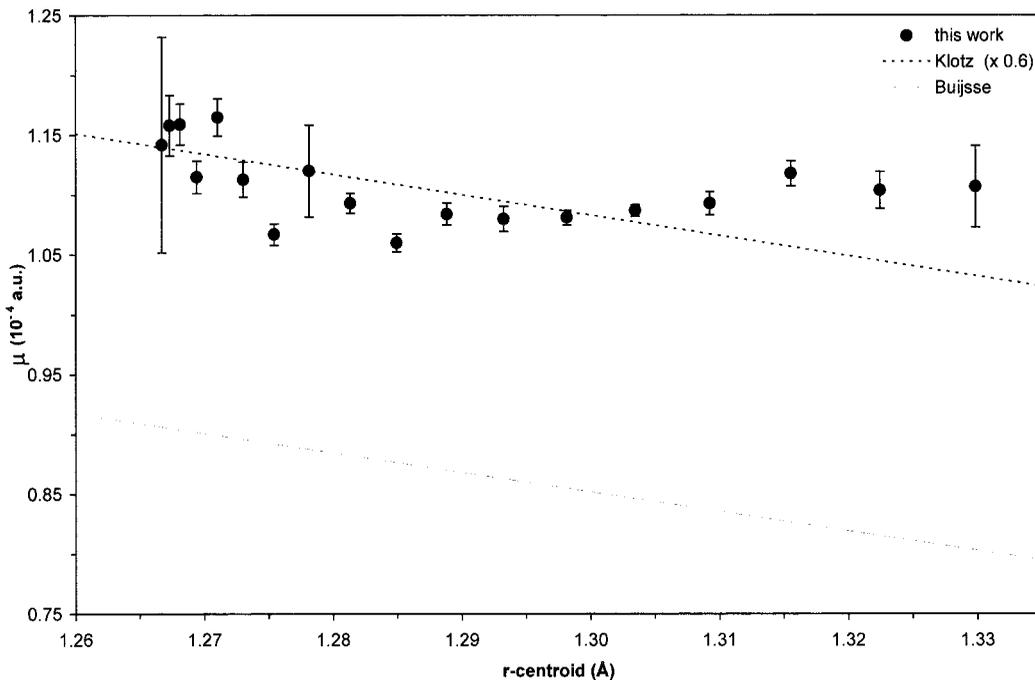
FIG. 8. Electronic transition moment μ for the c–X (v'–0) bands ($v' = 2$–19): this work; the r linear-dependent curve obtained by Buijsse *et al.* (*32*) from the CRDS oscillator strengths of Huestis *et al.* (*7*); the curve derived from the ab initio calculations of Klotz and Peyerimhoff (*30*) adjusted for comparison (see text).

value $U_3 \approx U_5$ of Klotz and Peyerimhoff (*30*). Once again, in order to present all sets of values on the same graph, the values of Klotz and Peyerimhoff (*30*) have been multiplied by 0.45. The effective electronic transition moments, calculated according to Buijsse *et al.* (*32*) at ambient temperature ($T = 293$ K; $J'' = 9$), are also given in Table 3c, together with the r-centroid values obtained from the RKR curves calculated from the data of Paper I for the A' state and the data of Amiot and Vergès (*31*) for the X state. The fit of the values gives the r-centroid (in Å) dependent variation of the electronic moment for 1.28 Å $< r <$ 1.33 Å:

$$M_{\text{eff}} = (6.19 - 3.04r)10^{-4} \text{ a.u.} \qquad [5]$$

IV. Cross Sections

From the band oscillator strengths determined (Tables 2a, 2b, and 2c) for the three transitions, effective vibrational cross sections for the levels below the dissociation threshold are calculated according to the expression derived by Smith (*36*):

$$\sigma(\nu_{v',0}) = \frac{2\pi e^2 N''}{mc^2} \frac{f_{v'0}}{G(v'+1) - G(v'-1)}. \qquad [6]$$

In Eq. [6], the term $2/[G(v'+1) - G(v'-1)]$ was defined by Smith (*36*) as the semiclassical density of vibrational states. To take into account the temperature, it is necessary to add a rotational energy contribution to the denominator. To do so, we

followed the same procedure as that of Buijsse *et al.* (*32*) using the modified expression

$$\sigma(\nu_{v'0}) = 1.77 \times 10^{-12} \frac{f_{v'0}}{\nu_{v'+1,0} - \nu_{v'-1,0}}, \qquad [7]$$

where $\nu_{v'+1,0}$ and $\nu_{v'-1,0}$ are effective band positions for $J'' = 9$, the most populated rotational level at 293 K. The $\nu_{v'0}$ values were taken as the $^QQ_{22}(9)$ line position (*13*) for the bands of the (A–X) and (A'–X) transitions; for the bands of the c–X transition, they were taken as the average value of the $R(9)$ and $P(9)$ line positions (*13*).

Figure 11 shows the calculated values of the cross sections of the Herzberg bands as a function of the wavenumbers. The summation of the three fitted curves (A–X + c–X + A'–X) leads to a total curve represented in Fig. 11. The curve extrapolated above the dissociation limit can be compared to the most recent cross-section values determined for the Herzberg continuum from: (a) previous measurements performed in Reims with the same absorption cell (*37*); (b) the measurements of Cheung *et al.* (*38*); (c) the measurements of Amoruso *et al.* (*39*); and (d) the combined results of Jenouvrier *et al.* (*37*) and Cheung *et al.* (*38*) given by Yoshino *et al.* (*24*).

The extrapolated curve of the discrete region is in good agreement with the continuum cross sections reported by Jenouvrier *et al.* (*37*) and Yoshino *et al.* (*24*).

The values of Amoruso *et al.* (*39*) are 20–25% lower than
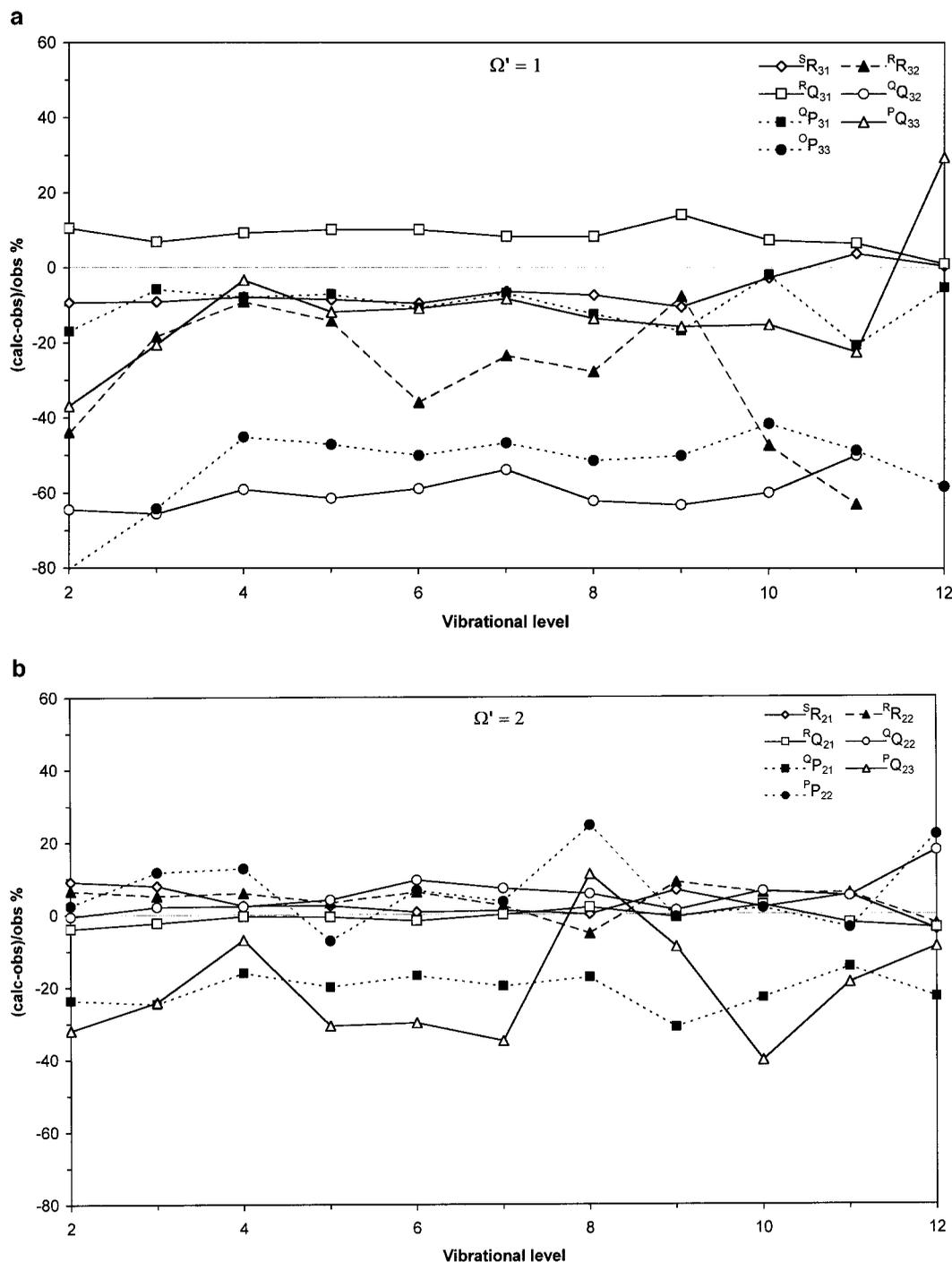
FIG. 9. (a) Percentage difference between the calculated and the observed integrated cross sections for the branches of the $A'-X$ ($v'-0$) subbands with Ω' = 1. (b) Percentage difference between the calculated and the observed integrated cross sections for the branches of the $A'-X$ ($v'-0$) subbands with Ω' = 2. (c) Percentage difference between the calculated and the observed integrated cross sections for the branches of the $A'-X$ ($v'-0$) subbands with Ω' = 3.

those of the combined results (*24*) and also appear to be lower than the extrapolated curve calculated from the effective vibrational cross sections of the $A-X$ transition alone.

Figure 12 also shows the curves for the contribution of the three transitions to the total absorption in the discrete region of the spectrum. The contribution of the $A-X$ transition increases with wavenumbers and reaches the value of 87% at 41 000 cm^{-1}. It should be larger above the dissociation limit as predicted by Buijsse *et al.* (*32*), who assumed a contribution of 94% at the maximum of the continuum at 50 500 cm^{-1}.
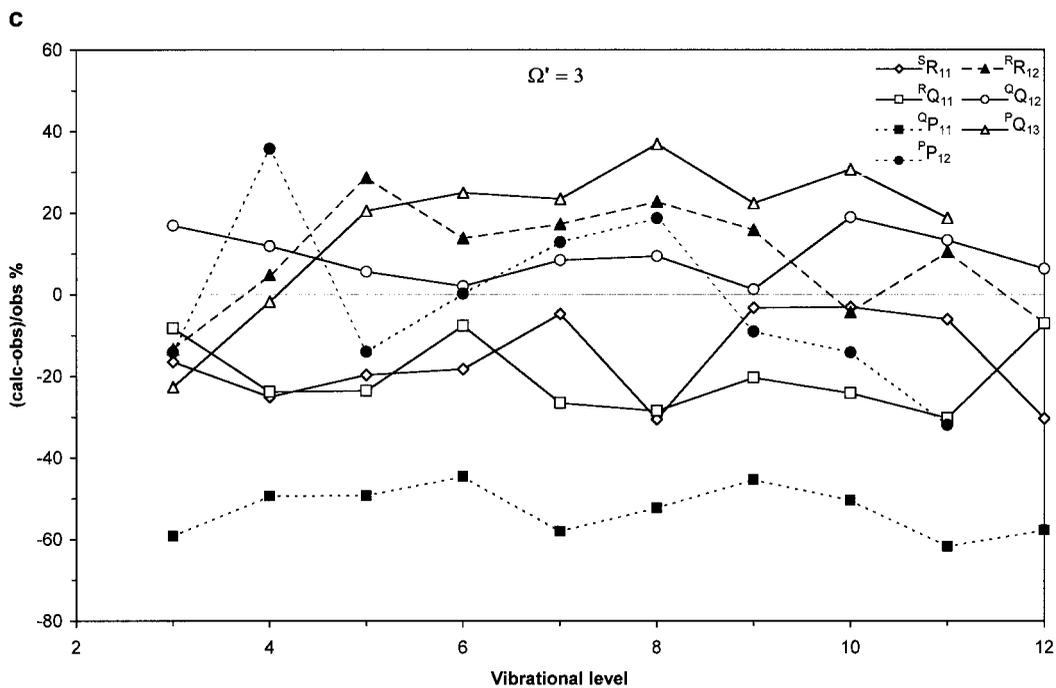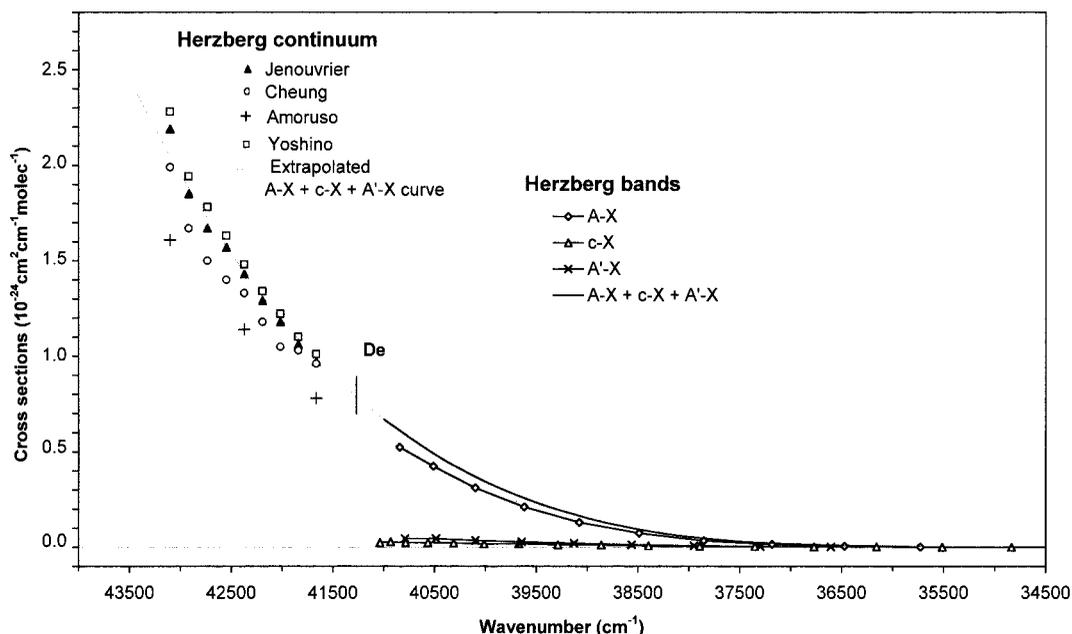
FIG. 9—*Continued*
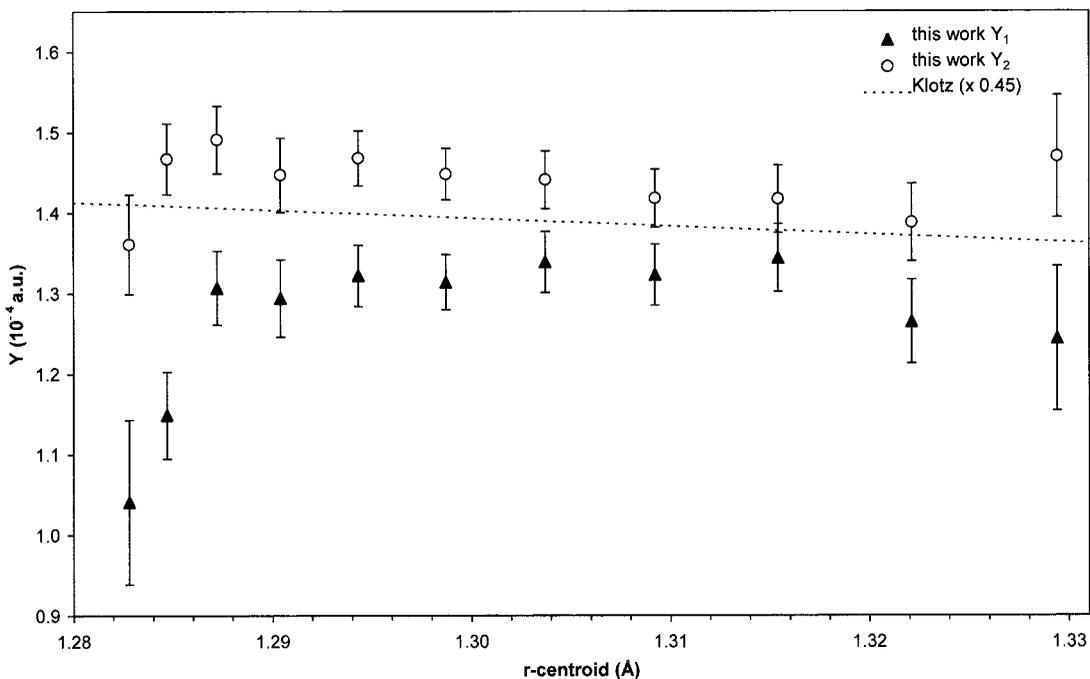
FIG. 10. Electronic transition moment parameters for the $A'-X$ ($v'-0$) bands ($v' = 2-12$): this work (Y_1 and Y_2 values); the curve derived from the ab initio calculation of Klotz and Peyerimhoff (*30*) for the parameter U3 adjusted for comparison (see text).

FIG. 11. Effective absorption cross sections for the Herzberg bands, determined from the vibrational oscillator strength densities: $A-X$ ($v'-0$) bands, $c-X$ ($v'-0$) bands, and $A'-X$ ($v'-0$) bands; the total absorption curve obtained by summing the fitted curves of the three discrete transitions is represented by a heavy line and the extrapolated curve by a thin line in the wavenumber region of the continuum; the absorption cross sections in the Herzberg continuum are those from Jenouvrier *et al.* (*37*), Cheung *et al.* (*38*), Amoruso *et al.* (*39*), and Yoshino *et al.* (*24*) (see text).

CONCLUSION

The study of the absorption intensities in the three Herzberg band systems has been carried out from experiments using conditions more extended than those of previous studies (*7, 10, 21*). Improved or new integrated cross-section values are given for the lines of the ($v'-0$) bands in the $A^3\Sigma_u^+ - X^3\Sigma_g^-$, $c^1\Sigma_u^- - X^3\Sigma_g^-$, and $A'^3\Delta_u - X^3\Sigma_g^-$ transitions having $v' = 0-11$, $v' =$
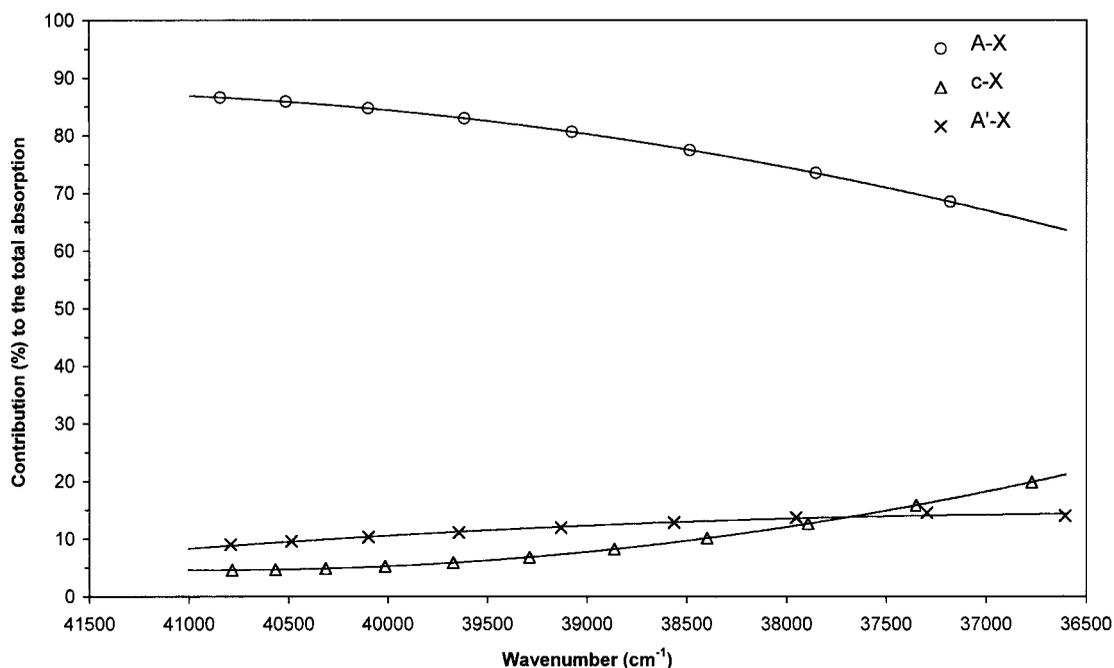
FIG. 12. Respective contributions of the three Herzberg band systems to the total absorption in the wavelength region of the discrete spectrum.

2–19, and $v' = 2$–12, respectively. Band oscillator strengths and effective transition moments depending slightly on the r-centroid values are calculated. Effective vibrational cross sections are determined for the three transitions. The individual contributions allow the derivation of a total absorption curve. Extrapolation of this curve beyond the dissociation limit is in good agreement with the absorption cross-section values previously obtained for the Herzberg continuum (*24, 37*).

The study of the intensity distribution in the branches of the three Herzberg band systems points out the need to improve the theoretical models for the $c\,^1\Sigma_u^- - X\,^3\Sigma_g^-$ and $A'\,^3\Delta_u - X\,^3\Sigma_g^-$ transitions. The accurate data set obtained in the present work should be a useful support for this purpose.

ACKNOWLEDGMENTS

REFERENCES

1. G. Herzberg, *Can. J. Phys.* **30,** 185–210 (1952).

2. G. Herzberg, *Can. J. Phys.* **31,** 657–669 (1953).

3. R. P. Saxon and T. G. Slanger, *J. Geophys. Res.* **91,** 9877–9879 (1986).

4. D. A. Ramsay, *Can. J. Phys.* **64,** 717–720 (1986).

5. P. M. Borrel, P. Borrel, and D. A. Ramsay, *Can. J. Phys.* **64,** 721–725 (1986).

6. B. Coquart and D. A. Ramsay, *Can. J. Phys.* **64,** 726–732 (1986).

7. D. L. Huestis, R. A. Copeland, K. Knutsen, T. G. Slanger, R. T. Jongma, M. G. H. Boogaarts, and G. Meijer, *Can. J. Phys.* **72,** 1109–1121 (1994).

8. T. G. Slanger, D. L. Huestis, P. C. Cosby, H. Naus, and G. Meijer, *J. Chem. Phys.* **105,** 9393–9402 (1996).

9. K. Yoshino, J. E. Murray, J. R. Esmond, Y. Sun, W. H. Parkinson, A. P. Thorne, R. C. M. Learner, and G. Cox, *Can. J. Phys.* **72,** 1101–1108 (1994).

10. K. Yoshino, J. R. Esmond, J. E. Murray, W. H. Parkinson, A. P. Thorne, R. C. Learner, and G. Cox, *J. Chem. Phys.* **103,** 1243–1249 (1995).

11. P. Bernath, M. Carleer, S. Fally, A. Jenouvrier, A. C. Vandaele, C. Hermans, M.-F. Mérienne, and R. Colin, *Chem. Phys. Lett.* **297,** 293–299 (1998).

12. S. Fally, M. Carleer, C. Hermans, A. C. Vandaele, B. Coquart, A. Jenouvrier, M.-F. Mérienne, and R. Colin, *in* "ASA Proceedings, Reims, 1999," pp. 153–156.

13. A. Jenouvrier, M.-F. Mérienne, B. Coquart, M. Carleer, S. Fally, A. C. Vandaele, C. Hermans, and R. Colin, *J. Mol. Spectrosc.* **198,** 136–162 (1999).

14. V. Hasson, R. W. Nicholls, and V. Degen, *J. Phys. B At. Mol. Phys.* **3,** 1192–1194 (1970).

15. V. Hasson and R. W. Nicholls, *J. Phys. B At. Mol. Phys.* **4,** 1778–1788 (1971).

16. B. R. Lewis and S. T. Gibson, *Can. J. Phys.* **68,** 231–237 (1990).

17. M. W. P. Cann and R. W. Nicholls, *Can. J. Phys.* **69,** 1163–1165 (1991).

18. D. R. Bates, *Planet. Space Sci.* **37,** 881–887 (1989).

19. Z. C. Bao, W. O. Yu, and J. R. Barker, *J. Chem. Phys.* **103,** 6–13 (1995).

20. J. P. England, B. R. Lewis, and S. T. Gibson, *Can. J. Phys.* **74,** 185–193 (1996).

21. K. Yoshino, J. R. Esmond, W. H. Parkinson, A. P. Thorne, R. C. Learner, and G. Cox, *J. Chem. Phys.* **111,** 2960–2967 (1999).

22. T. G. Slanger and D. L. Huestis, *J. Geophys. Res.* **86,** 3551–3554 (1981).

23. C. M. L. Kerr and J. K. G. Watson, *Can. J. Phys.* **64,** 36–44 (1986).

24. K. Yoshino, A. S. C. Cheung, J. R. Esmond, W. H. Parkinson, D. E. Freeman, S. L. Guberman, A. Jenouvrier, B. Coquart, and M.-F. Mérienne, *Planet. Space Sci.* **36,** 1469–1475 (1988).

25. J. P. Lux and A. Jenouvrier, *Rev. Phys. Appl.* **20,** 869–875 (1985).

26. M. Carleer, *in* "12th Symposium on High Resolution Molecular Spectroscopy, Dijon, France, 9–13 Sept., 1991."

27. V. P. Bellary and T. K. Balasubramanian, *J. Quant. Spectrosc. Radiat. Transfer* **45,** 283–289 (1991).

28. R. D. Present, *Phys. Rev.* **48,** 140–148 (1935).

29. D. L. Huestis and T. G. Slanger, *in* "38th Symposium on Molecular Spectroscopy, Colombus, 1983," Paper WF 3.

30. R. Klotz and S. Peyerimhoff, *Mol. Phys.* **57,** 573–594 (1986).

31. C. Amiot and J. Vergès, *Can. J. Phys.* **59,** 1391–1398 (1981).

32. B. Buijsse, W. J. van der Zande, A. T. J. B. Eppink, D. H. Parker, B. R. Lewis, and S. T. Gibson, *J. Chem. Phys.* **108,** 7229–7243 (1998).

33. J. K. G. Watson, *Can. J. Phys.* **46,** 1637–1643 (1968).

34. V. P. Bellary and T. K. Balasubramanian, *J. Mol. Spectrosc.* **126,** 436–442 (1987).

35. V. P. Bellary and T. K. Balasubramanian, *J. Mol. Spectrosc.* **148,** 270–273 (1991).

36. A. L. Smith, *J. Chem. Phys.* **55,** 4344–4350 (1971).

37. A. Jenouvrier, B. Coquart, and M.-F. Merienne, *J. Quant. Spectrosc. Radiat. Transfer* **36,** 349–364 (1986).

38. A. S.-C. Cheung, K. Yoshino, W. H. Parkinson, S. L. Guberman, and D. E. Freman, *Planet. Space Sci.* **34,** 1007–1021 (1986).

39. A. Amoruso, L. Crescentini, M. S. Cola, and G. Fiocco, *J. Quant. Spectrosc. Radiat. Transfer* **56,** 145–152 (1996).